

BVI Photometric Variability Survey of M3.

J. D. Hartman¹, J. Kaluzny², A. Szentgyorgyi¹ & K. Z. Stanek¹

`jhartman@cfa.harvard.edu`, `jka@camk.edu.pl`, `aszentgyorgyi`, `kstanek@cfa.harvard.edu`

ABSTRACT

We have conducted a three band (*BVI*) variability survey of the globular cluster M3. This is the first three band survey of the cluster using modern image subtraction techniques. Observations were made over 9 nights in 1998 on the 1.2 m. telescope at the F. L. Whipple Observatory in Arizona. We present photometry for 180 variable stars in the M3 field, of which 12 are newly discovered. New discoveries include six SX Phe type variables which all lie in the blue straggler region of the color magnitude diagram, two new first overtone RR Lyrae, a candidate multi-mode RR Lyrae, a detached eclipsing binary, and two unclassified variables. We also provide revised periods for 52 of the 168 previously known variables that we observe. The catalog and photometry for the variable stars are available via anonymous ftp at <ftp://cfa-ftp.harvard.edu/pub/kstanek/M3/>.

Subject headings: globular clusters: individual (M3) — binaries: eclipsing — delta Scuti — stars: variables: other — surveys

1. Introduction

The globular cluster M3 (NGC 5272) is one of the most studied clusters in the Galaxy. Since the work of Bailey (1913) and Shapley (1914), there have been numerous surveys for photometric variability in the cluster. In 1973, Sawyer-Hogg compiled the most complete catalog of variables in the cluster prior to the modern era. Recently Bakos, Benko, & Jurcsik (2000) compiled a catalog of 274 variable stars in the cluster, and published improved identification and astrometry for them. M3 is particularly known for containing the largest number of RR Lyrae variables, with more than 182 such stars (Clement et al. 2001). Many groups have focused on studying the population of RR Lyrae variables. Corwin et al. (2001) and Clementini et al. (2004) have published a catalog of 222 confirmed or suspected RR Lyrae variables, and have provided a detailed analysis of the 8 known double-mode RR Lyraes (RRd). Other surveys have focused specifically on searches for variability in blue straggler stars (BSS), notably Kaluzny et al. (1998) discovered only one SX Phe star out

¹Harvard-Smithsonian Center for Astrophysics, 60 Garden St., Cambridge, MA 02138, USA

²Nicolaus Copernicus Astronomical Center, ul. Bartycka 18, 00-716 Warszawa, Poland

of 25 monitored BSS. They also discovered a contact binary star near the base of the red giant branch.

In this contribution we present the data from a *BVI* variability survey of the cluster performed in the spring of 1998. This is the first three band survey of the cluster using modern image subtraction techniques. New results include the discovery of 6 new SX Phe variables, 2 new first-overtone RR Lyraes, a candidate multi-mode RR Lyrae, a detached eclipsing binary, and 2 new variables that we do not classify. We also provide revised periods for 52 of the 168 previously known variables that we observe.

We describe our observations and data reduction in the following section. In §3 we present the catalog of variables, in §4 we analyze the light curve of the eclipsing binary NV296, in §5 we briefly describe the population of variables using color magnitude diagrams, and in §6 we discuss the results.

2. Observations and Data Reduction

The observations were made at the F. L. Whipple Observatory (FLWO) 1.2 m telescope using the 4-Shooter CCD mosaic containing four thinned, back-side-illuminated, AR-coated Loral 2048x2048 CCDs. The camera has a pixel scale of $0''.333 \text{ pixel}^{-1}$ and a field of view (FOV) of $11'4 \times 11'4$ for each chip. We obtained observations on 9 nights between the dates of April 16-20, 1998 and May 28-31, 1998. These observations consist of 4 x 300 s, and 67 x 420 s *B*-band exposures, 14 x 240 s, 198 x 300 s, and 13 x 450 s *V*-band exposures and 4 x 180 s, and 72 x 240 s *I*-band exposures. The sampling cadence was as low as 7 minutes, allowing for the detection of very short period SX Phe variables. The center of M3 at $(\alpha, \delta) = (13^{\text{h}}42^{\text{m}}11^{\text{s}}.2, +28^{\circ}22'32'')$ (J2000.0) was positioned in the lower, right corner of chip 3. A mosaic of all four chips is shown in Fig 1.

The preliminary CCD reductions were performed using the standard routines in the IRAF CCDPROC package¹.

To obtain photometry we used the image subtraction techniques due to Alard & Lupton (1998; also Alard 2000) as implemented in the ISIS 2.1² package. To detect variables we first took the absolute value of all the subtracted images and stacked them to form a single image. We then searched this image for strong point sources, identifying these as variables. We obtained light curves only for sources identified as variable in this way by performing weighted-aperture photometry on the subtracted images. This procedure provides differential photometry in Analog-to-Digital Units (ADUs), to convert to magnitudes we obtained profile photometry for the stars

¹IRAF is distributed by the National Optical Astronomy Observatories, which is operated by the Association of Universities for Research in Astronomy, Inc., under agreement with the National Science Foundation.

²ISIS package is available from C. Alard's web-site at <http://www2.iap.fr/users/alard/package.html>

in our field using the DAOPHOT/ALLSTAR package (Stetson 1987, 1991). As a sanity check, we also generated light curves using profile photometry which resulted in generally worse precision and yielded no additional variables. The method that we have just described is the same technique used by Kaluzny et al. (2001); the procedure is discussed in more detail in that paper.

We also generated light curves for blue straggler stars, examining them individually for variability. We identified a handful of low-amplitude (0.04 mag) SX Phe variables in this fashion.

To transform our light curves to standard BVI magnitudes we observed a total of 128 stars from 22 Landolt (1992) fields so that the transformation for each chip utilized typically 30 stars from 5 fields. The airmass of these observations ranged from 1.08 to 1.93. The resulting uncertainty in the zero-point of our observations is 0.02 magnitudes. As a consistency check we calculated the median colors for the turnoff stars independently for each chip. The results shown in Table 1 are consistent with an uncertainty of 0.02 magnitudes.

We obtained astrometry for the variables by first matching to the catalog of Bakos et al. (2000). We used at least 10 preliminary matches on each chip to obtain the transformation between rectangular and equatorial coordinates. The residuals of the matched stars were less than $0''.1$. Using the RA/DEC from this transformation we proceeded to match our sources to the Two Micron All Sky Survey (*2MASS*; Skrutskie et al. 1997) point-source catalog using a matching radius of $0''.7$ for a total of 98 matches. The median residual was $0''.43$. All but three of these matches are RR Lyrae. Both of the unclassified newly discovered variables and one of the newly discovered SX Phe variables matched to sources in *2MASS*. Figure 2 shows the location of 93 of the matched sources on the *2MASS J* vs. $J - K$ color-magnitude-diagram (CMD) for M3. The five matched sources not shown in this figure were missing K photometry. The fact that all but a few sources lie clumped near a region of constant J (the horizontal branch) suggests that these matches to RR Lyrae are correct, with the scatter likely due to variability of the RR Lyrae and blending with nearby sources. In Figure 3 we plot the position on the sky of all RR Lyrae in our catalog, together with the positions of those that match to *2MASS*. From this figure it is clear that the non-matches are due to incompleteness in the *2MASS* catalog near the crowded center of the globular cluster.

3. Catalog of Variables

Following the above procedures we identify 180 variable sources of which 12 are newly identified as variables. The newly identified variables include 6 new SX Phe stars, 2 first overtone RR Lyrae (RR1), a candidate multi-mode RR Lyrae (RR01), one detached eclipsing binary (EB), and 2 unclassified variables. We also provide revised periods for 52 of the known variables. The revisions were determined based on visual comparisons between the light curves phased with the published period and the light curves phased with the period calculated using the Schwarzenberg-Czerny (1996) algorithm. We consider the period to be necessary of revision if the published period is incompatible with the observed light curve given the formal errors from the photometry. We have

recovered one of the previously identified SX Phe stars (V237), we note however that the coordinates given for this variable appear to have been switched with the coordinates for V238 in the discovery paper by Kaluzny et al. (1998), this error has been propagated through the catalogs of Bakos et al. (2000) and Clement et al. (2001), we also revise the period for this variable. Finding charts for the newly discovered variables are shown in Figure 4. A machine-readable version of the catalog, as well as V , B , I , $B - V$ and $V - I$ light curves for the variable stars are available via anonymous ftp³. We present the catalog in Tables 3 and 4, the columns are as follows:

- ID : The ID number of the variable. V1-V285 is taken from Clement et al. (2001). New identifications are denoted by “NV.” The ID number roughly corresponds to discovery order.
- $2MASS\text{-}flag$: Integer denoting whether or not the variable matched to a $2MASS$ source. The flag is 0 for no match, and 1 for a match.
- RA : Right ascension for epoch J2000.0. This value is taken from the $2MASS$ catalog for sources with a $2MASS$ match, otherwise it is obtained from the rectangular to equatorial transformation derived using the Bakos et al. (2000) catalog.
- DEC : Declination for epoch J2000.0. This value is taken from the $2MASS$ catalog for sources with a $2MASS$ match, otherwise it is obtained from the rectangular to equatorial transformation derived using the Bakos et al. (2000) catalog.
- V_{flag} : Integer denoting the type of V-band observations. Values are 1 for observations that could be converted to magnitudes or 2 for observations that were left in differential count units.
- B_{flag} : Integer denoting the type of B-band observations. Values are 0 for no B-band detection, 1 for observations that could be converted to magnitudes, or 2 for observations that were left in differential count units.
- I_{flag} : Integer denoting the type of I-band observations. Values are 0 for no I-band detection, 1 for observations that could be converted to magnitudes, or 2 for observations that were left in differential count units.
- A_V : Observed full-amplitude in V-band, defined to be the faintest observed magnitude minus the brightest observed magnitude on the cleaned light curve.
- $\langle V \rangle$: Flux averaged mean V magnitude of the star. For the eclipsing binary this is the out of eclipse magnitude determined with EBOP(see §4).
- A_B : Observed full-amplitude in B-band, defined to be the faintest observed magnitude minus the brightest observed magnitude on the cleaned light curve.

³<ftp://cfa-ftp.harvard.edu/pub/kstanek/M3/>

- $\langle B \rangle$: Flux averaged mean B magnitude of the star. For the eclipsing binary this is the out of eclipse magnitude determined with EBOP(see §4).
- A_I : Observed full-amplitude in I-band, defined to be the faintest observed magnitude minus the brightest observed magnitude on the cleaned light curve.
- $\langle I \rangle$: Flux averaged mean I magnitude of the star. For the eclipsing binary this is the out of eclipse magnitude determined with EBOP(see §4).
- *Period*: The observed best period of variability in days. This was derived using the ANOVA statistic of Schwarzenberg-Czerny (1996). In cases where aliasing allowed for a number of acceptable periods, we chose the period corresponding to the peak in the periodogram nearest to the published period, where available.
- *Published Period*: The published period for the star taken from Clementini et al. (2004), Corwin & Carney (2002) or Clement et al. (2001) in that order of priority.
- *Period Revision Flag*: Integer denoting whether or not the observed best period should be taken as a revision of the published period. This determination is based on a visual comparison between the light curve phased with the published period and the light curve phased with the observed best period. Values are 1 for a revision, and 0 for no revision.
- *JD of minimum V*: Julian Date (in 2450000) of the first minimum in V-band to occur after the first observation. This field is null for unclassified variables.
- *Phase of minimum B*: Phase of the minimum in B-band, where 0 phase is set to the minimum in V-band.
- *Phase of minimum I*: Phase of the minimum in I-band, where 0 phase is set to the minimum in V-band.
- *Classification*: Classification of variability, the symbols are as follows:
 - RR0: fundamental mode RR Lyr (RRab).
 - RR1: first overtone RR Lyr (RRc).
 - RR01: candidate multi-mode RR Lyr (RRd). Note that the possible presence of multiple periods was determined by eye and was not the result of a systematic search.
 - SXP: SX Phe type variable.
 - N/A: Unclassified variable.
 - EB: Eclipsing binary.
- *Remarks*: Here we denote the possible presence of multiple modes (mp) for SXP variables as well as the presence of the Blazhko effect (Bl) within the observations.

Figure 5 shows the V -band, $B - V$ and $V - I$ light curves for 12 of the 130 previously identified variables in the catalog for which these 3 measurements are available. We display V , $B - V$ and $V - I$ light curves, where available, for the 2 unclassified new variables and the 3 new RRPs in Figure 6 and light curves for the 6 new SX Phe variables in Figure 7. The BVI light curves for the eclipsing binary (NV297) are shown in Figure 8 together with a model fit.

4. Analysis of the Eclipsing Binary NV296

Parameters for the eclipsing binary NV296 were determined using the Eclipsing Binary Orbit Program (EBOP) model for detached eclipsing binaries (Nelson & Davis 1972; Popper & Etzel 1981) (see Figure 8). The first step was to obtain a fit to the V -band light curve. In doing so we varied the luminosity ratio, the radius of the primary, the inclination of the orbit, and the out-of-eclipse luminosity. We then obtained a second fit varying the ratio of the radii in place of the radius of the primary. We found empirically that the solution would not converge when the radius of the primary and the ratio of the radii were allowed to vary simultaneously. We held the mass ratio fixed at 1.0, and assumed that gravity darkening and the reflection effect were negligible. Because the period is relatively short (0.445955 days) we assumed that the orbits would have circularized, so we held the eccentricity fixed to 0. We note that when we allowed this parameter to vary the results were consistent with $e = 0$. Having obtained a model for the V -band light curve, we proceeded to fit a model to the B -band light curve assuming the same orbital parameters and radii from the V -band model. We did not analyze the I -band light curve since noise and poor phase coverage during the eclipses conspired to prevent us from obtaining an acceptable fit.

Without spectra it is difficult to constrain the spectral types and luminosity classes of the components, and hence the limb darkening coefficients. As a preliminary analysis we fixed the limb darkening coefficients for both components to 0.57 in V and 0.72 in B , which is consistent with an F2V star in the limb darkening tables from Claret & Gimenez (1990). We caution that the results from this fit should be treated as preliminary until spectra can be obtained for this variable..

The parameters from the best fit model are shown in Table 2. To test the effect of the unconstrained mass ratio on the fit, we obtained an independent model assuming a mass ratio of 0.7. The parameters for this model are also shown in Table 2, we note that the results appear to be consistent, in particular the position of the components on the CMD is unaffected by the mass ratio. We find that the primary has $B - V = 0.349 \pm 0.042$ mag, and $V = 19.331 \pm 0.028$ mag, while the secondary has $B - V = 0.395 \pm 0.064$ mag, and $V = 19.747 \pm 0.042$ mag. The errors listed here and in Table 2 are propagated from the standard errors produced by the EBOP fits, we caution that for all parameters except the color these errors are likely to be optimistic. In the case of the $B - V$ colors the errors listed are calculated assuming B and V are uncorrelated when in reality the two magnitudes will be correlated as a result of the fitting procedure. We note that for three different choices of the limb darkening coefficients $B - V$ changed by less than a percent for both components whereas the other parameters varied by amounts consistent with the standard errors.

5. Color Magnitude Diagrams

In Figures 9 and 10 we plot the $B - V$ vs. V and $V - I$ vs. V CMDs for the cluster. In these figures we use filled circles to show RR Lyr variables, open squares for SXP variables, stars for unclassified variables and open triangles for the two components of the EB. Blue straggler stars that were examined for variability are shown with filled triangles. Note that these stars were selected based on their position in the $B - V$ CMD. Where available, the locations of these stars in the $V - I$ CMD are also shown.

The SXP variables for which colors could be obtained all lie within the blue straggler region of the CMD as a result of our selection procedure. Although their location on the CMD may indicate that these variables are indeed likely members of the cluster, one must be cautious in such claims following the identification with quasars of three variables in the M3 field lying in the blue straggler region of the CMD (Meusinger, Sholz & Irwin, 2001).

The components of the eclipsing binary NV296 appear to lie near the ZAMS at a distance of $(m - M)_V = 15.04$ mag (Harris 1996). The photometry for the primary is consistent with an F2V dwarf, and the secondary is consistent with an F3-4V dwarf. If the eclipsing binary is indeed a member of the cluster then both components (particularly the primary) appear to lie slightly below the cluster main sequence, closer to the ZAMS for the cluster.

The location of the unclassified variables on the CMD is completely uncertain since we have not observed a full period for either of these stars.

To further study the RR Lyr population we plot the horizontal branch regions of the CMDs in detail in Figures 11 and 12. Here we distinguish between the types of RR Lyr variables using filled circles for RRab, open circles for RRc and open stars for RRd candidates. The evolution from RRab to RRc along the horizontal branch is clearly demonstrated in the CMD for M3. We note that some RR Lyrae may appear to lie outside of the instability strip as a result of uncertainties in their colors. We also note that blending near the center of the cluster may cause a few variables to appear artificially bright.

6. Discussion

There has been a great deal of interest in studying the variability of BSS in globular clusters. A number of globular clusters show a substantial population of variable blue stragglers. Gilliland et al. (1998) found that 9 out of 47 monitored BSS in 47 Tucanae showed variability above 0.02 mag. Recently Kaluzny et al (2004) identified 35 new SX Phe variables in ω Centauri. However, despite having a sizeable population of BSS, Kaluzny et al. (1998) found only a single SX Phe star in M3. We confirm the relative under-abundance of SX Phe stars in M3, finding only 7 variables out of 122 monitored BSS. We note that with image subtraction we would have been able to detect single-mode, short-period variability in the monitored BSS with amplitudes greater than 0.02 magnitudes

(see for example NV289 in Figure 5).

Eclipsing binaries are another interesting target for globular cluster variability surveys. Besides the possibility that binaries play an important role in the dynamical evolution of globular clusters (Hut et al. 1992) and the formation of the BSS (Leonard 1989; Leonard & Fahlman 1991), eclipsing binaries can also be used as a tool to determine accurate ages and distances to the clusters (Paczynski 1997; see Kaluzny et al. 2004 for a discussion of a systematic program to search for detached eclipsing binaries in nearby globular clusters). The location of the components of NV296 on the CMD suggests that the binary may indeed be a member of the cluster. If it is a member, then there must be some mechanism that has allowed the components to avoid evolution into a giant. One hypothesis may be mass transfer onto the primary, however the fact that the light curve seems well fit by a detached eclipsing binary model suggests that mass transfer is not currently occurring at a significant rate. Moreover, the secondary star itself appears to be younger than other F3-4V stars in the cluster. It is necessary to obtain spectra for this system before anything more can be said about its membership. If it is a member, then spectra will be useful in determining the masses of the components.

As mentioned in the introduction, many of the recent studies of M3 have focused on the RR Lyrae population. Most recently Cacciari, Corwin & Carney (2004) used data from previous *BVI* surveys to conduct a detailed analysis of the RR Lyrae population in M3. Other authors have pointed to inconsistencies between existing models for horizontal branch evolution and the observed population (Catelan 2004; Clementini et al. 2004 discuss the observation of rapid evolution among the double mode RR Lyrae). Although we do not perform a systematic analysis of the RR Lyrae population, the data that we present should be useful for further investigations of these stars.

We gratefully acknowledge G. Pojmanski for his excellent “lc” program, J. Devor for his period-finding code, and G. Torres for his help with the EBOP routine. This research has made use of the SIMBAD database, operated at CDS, Strasbourg, France. It has also made use of images from the Digitized Sky Survey which were produced at the Space Telescope Science Institute under U.S. Government grant NAG W-2166. The images of the DSS are based on photographic data obtained using the Oschin Schmidt Telescope on Palomar Mountain and the UK Schmidt Telescope. The plates were processed into the present compressed digital form with the permission of these institutions. JDH is funded by a National Science Foundation Graduate Student Research Fellowship.

REFERENCES

Alard, C., Lupton, R. 1998, ApJ, 503, 325

Alard, C. 2000, A&AS, 144, 363

Bailey, S. 1913, Obs, 78, 1

- Bakos, G. A., Benko, J. M. & Jurcsik, J. 2000, AcA, 50, 221
- Cacciari, C., Corwin, T. M. & Carney, B. W. 2004, AJ, in press (astro-ph/0409567)
- Catelan, M. 2004, ApJ, 600, 409
- Claret, A. & Gimenez, A. 1990, A&A, 230, 412
- Clement, C., et al. 2001, AJ, 122, 2587
- Clementini, G., Corwin, T. M., Carney, B. W., & Sumerel, A. N. 2004, AJ, 127, 938
- Corwin, T. M., & Carney, B. W. 2001, AJ, 122, 3183
- Gilliland, R. L., et al. 1998, ApJ, 507, 818
- Harris, W. E. 1996, AJ, 112, 1487
- Hut, P., et al. 1992, PASP, 104, 981
- Kaluzny, J., Hilditch, R. W., Clement, C., & Rucinski, S. M. 1998, MNRAS, 296, 347
- Kaluzny, J., Olech, A., & Stanek, K. Z. 2001, AJ, 121, 1533
- Kaluzny, J., Olech, A., Thompson, I. B., Pych, W., Krzeminski, W., & Schwarzenberg-Czerny, A. 2004, A&A, in press (astro-ph/0406456)
- Landolt, A. 1992, AJ, 104, 340
- Leonard, P. J. T. 1989, AJ, 98, 217
- Leonard, P. J. T., & Fahlman, G. G. 1991, AJ, 102, 994
- Meusinger, H., Scholz, R. D., & Irwin, M. 2001, IBVS, 5037, 1
- Nelson, B., & Davis, W. D. 1972, ApJ, 174, 617
- Paczyński, B. 1997, Space Telescope Science Series, “The Extragalactic Distance Scale”, ed. M. Livio, Cambridge University Press, 273
- Popper, D. M., & Etzel, P. B. 1981, AJ, 86, 102
- Sawyer-Hogg, H. 1973, Publ. David Dunlop Obs., 3, 1
- Schwarzenberg-Czerny, A. 1996, ApJ, 460, 107
- Shapley, H. 1914, ApJ, 40, 443
- Skrutskie, M. F., et al. 1997, The Impact of Large-Scale Near-IR Sky Surveys, ed. F. Garzón, N. Epchtein, A. Omont, B. Burton, & P. Persei (Dordrecht: Kluwer), 25
- Stetson, P. B. 1987, PASP, 99, 191
- Stetson, P. B. 1991, ASP Conf. Ser. 25, Astronomical Data Analysis, Software and Systems I, ed. D. M. Worrall, C. Biemesderfer, & J. Barnes (San Francisco: ASP), 297

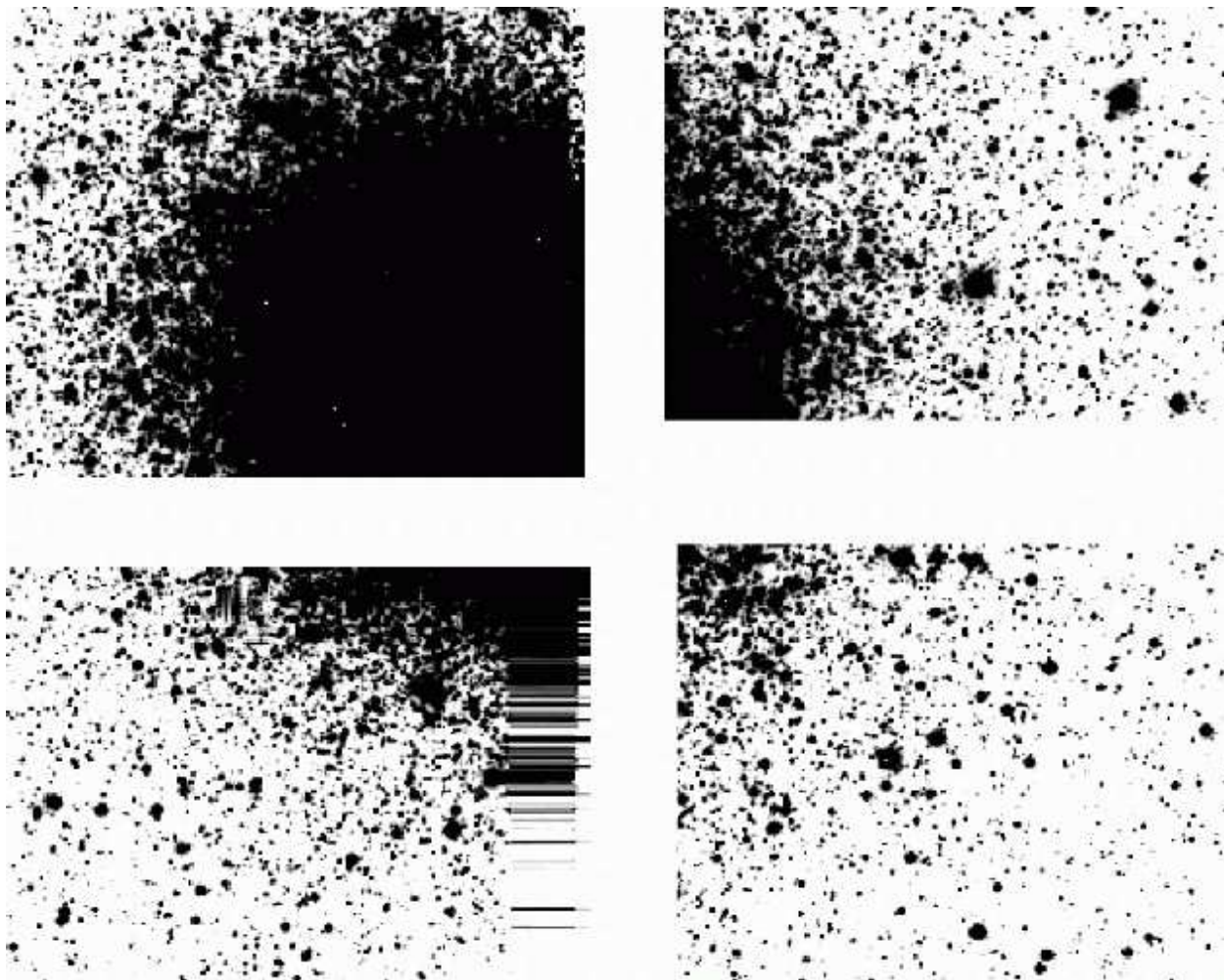


Fig. 1.— A mosaic of the four chips showing the position of M3 within the $18' \times 18'$ field of view. The horizontal lines in chip 2 are the result of running fixpix across a number of bad columns.

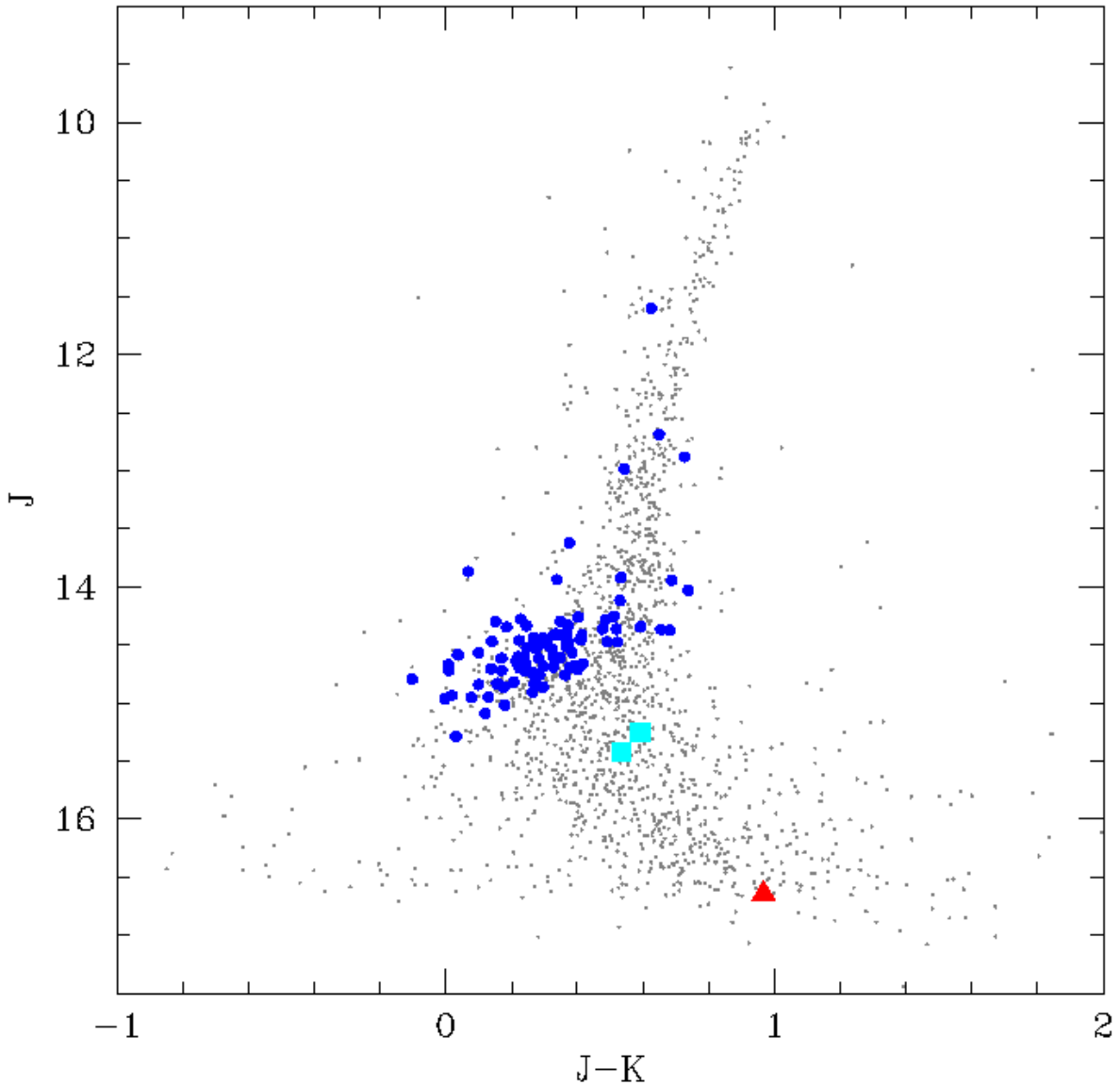


Fig. 2.— *2MASS J* vs. $J - K$ CMD for the globular cluster M3. The filled circles denote *2MASS* sources that match to RR Lyrae in our catalog, filled squares denote sources that match to unclassified variables in our catalog, and the filled triangle shows the source that matched to an SX Phe variable in our catalog. The fact that the RR Lyrae cluster in a single region of the CMD confirms that these matches to *2MASS* are real.

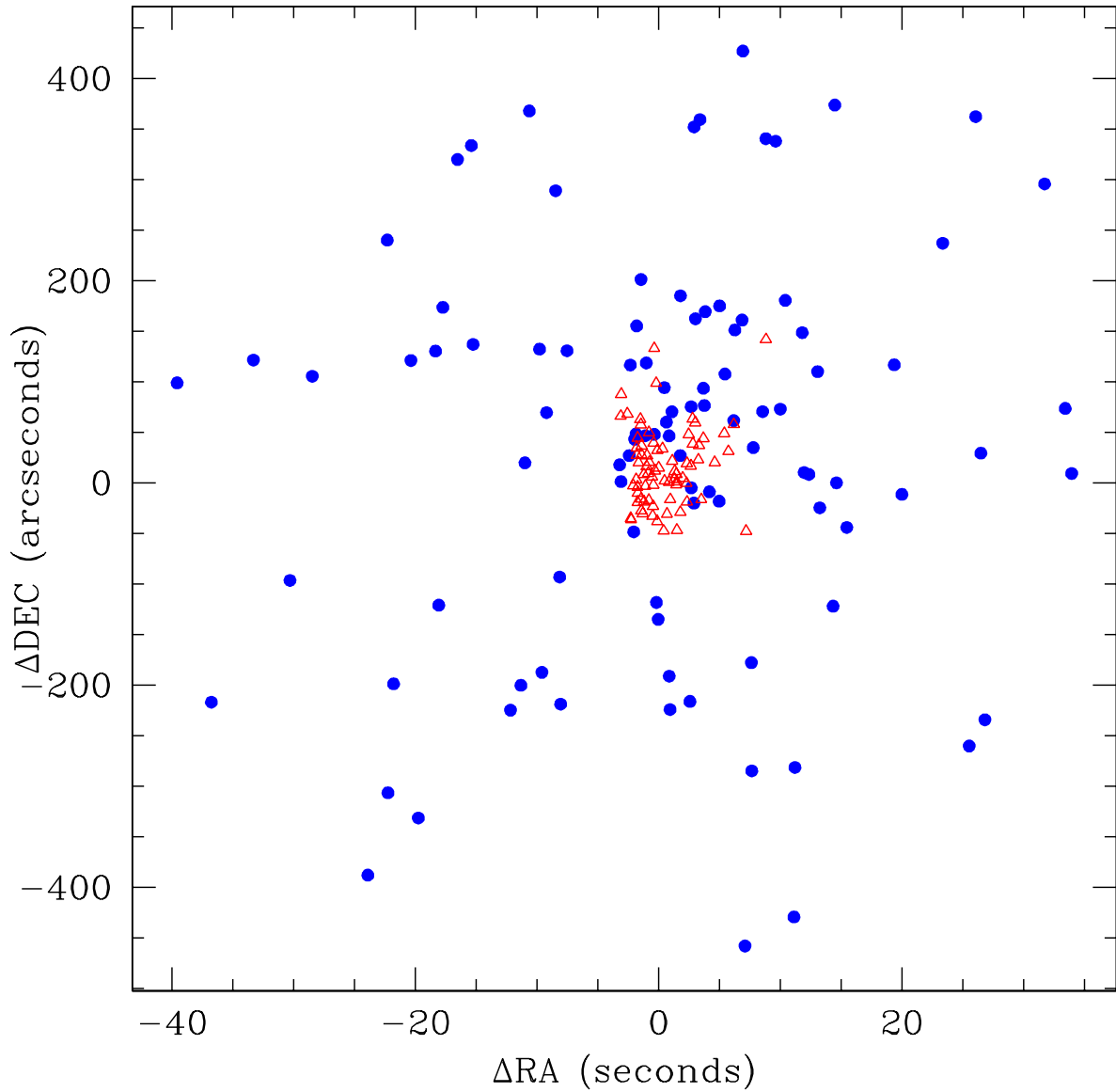


Fig. 3.— Distance from the center of the cluster of RR Lyrae that had matches to *2MASS* (filled circles) as well as those that did not (open triangles). From this it is clear that non-matches are the result of incompleteness in the *2MASS* catalog in the crowded center of the cluster.

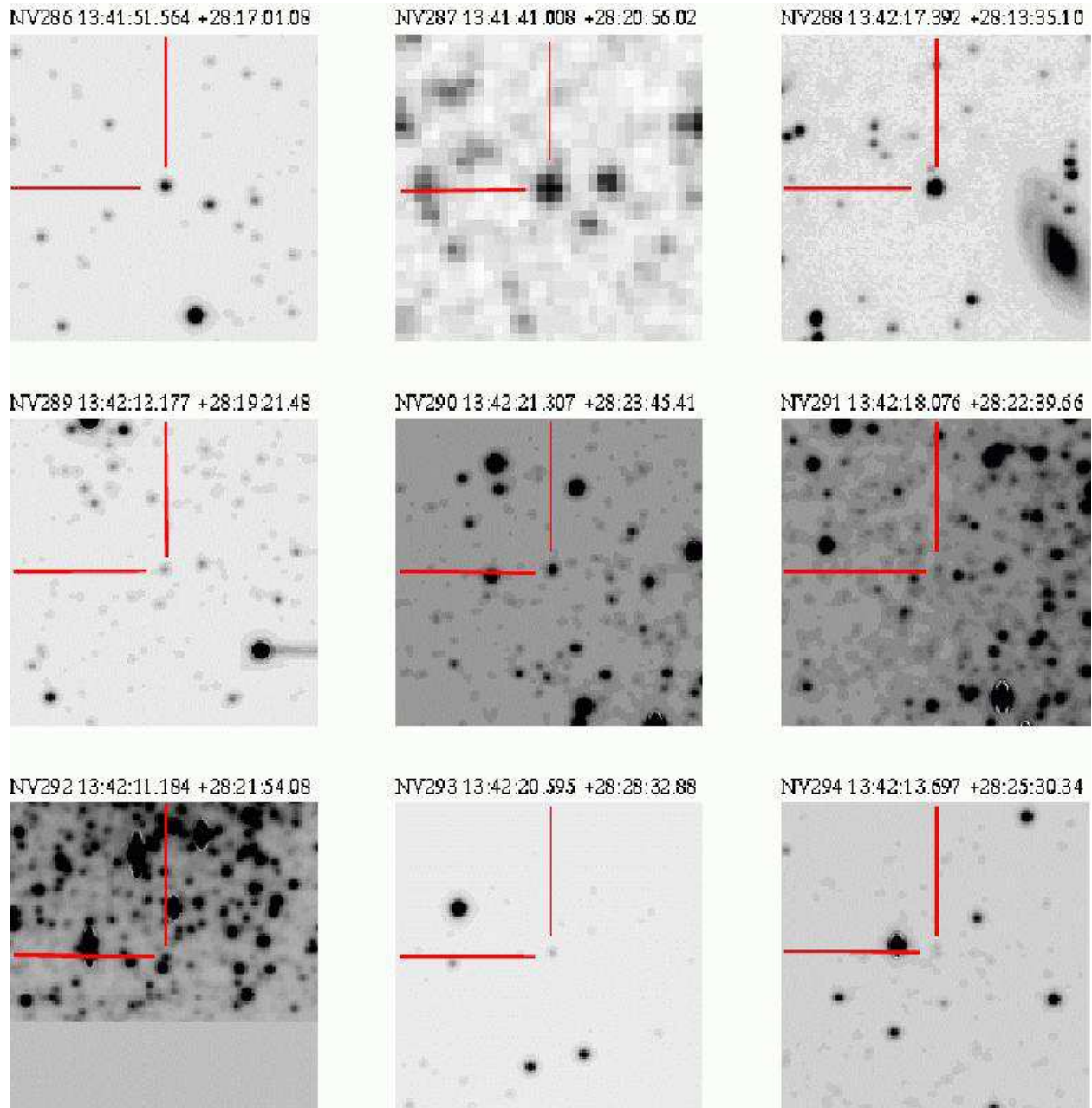


Fig. 4.— 1'x1' finding charts for the 13 newly discovered variables. The chart for NV287 is from the DSS, all other images are taken from our observations.

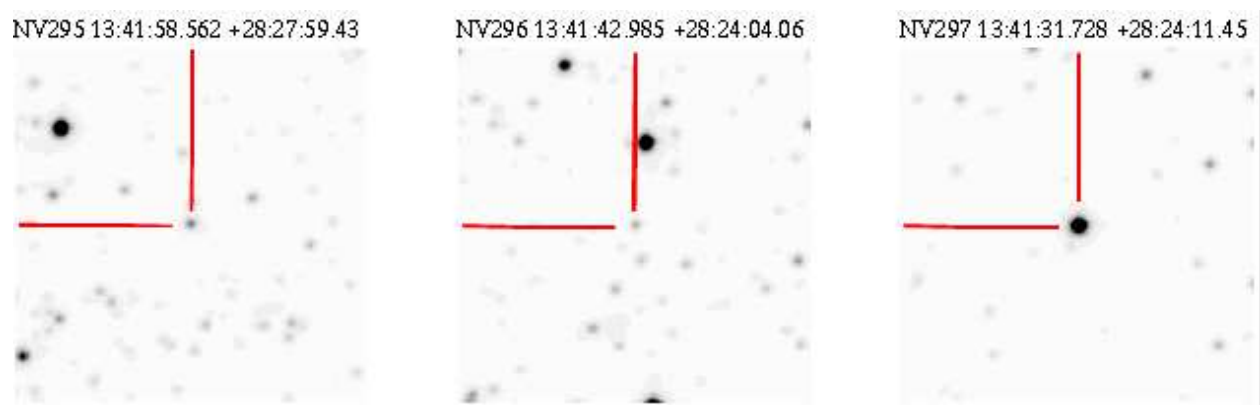


Fig. 4.— *Continued.*

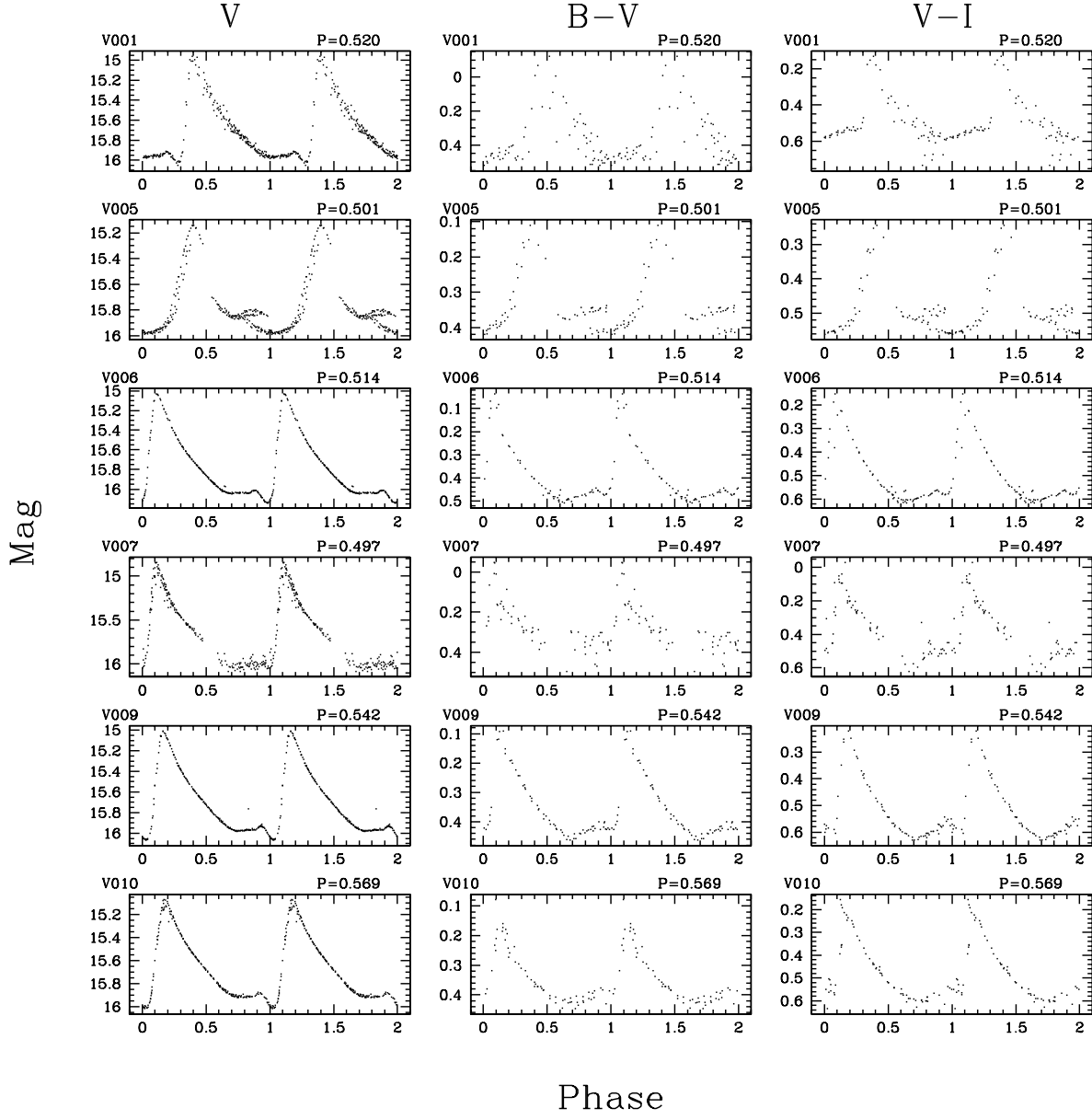


Fig. 5.— V, B-V and V-I light curves for 12 of the 130 previously identified variables for which all three of these measurements were available. Phase = 0 is set to the minimum in V.

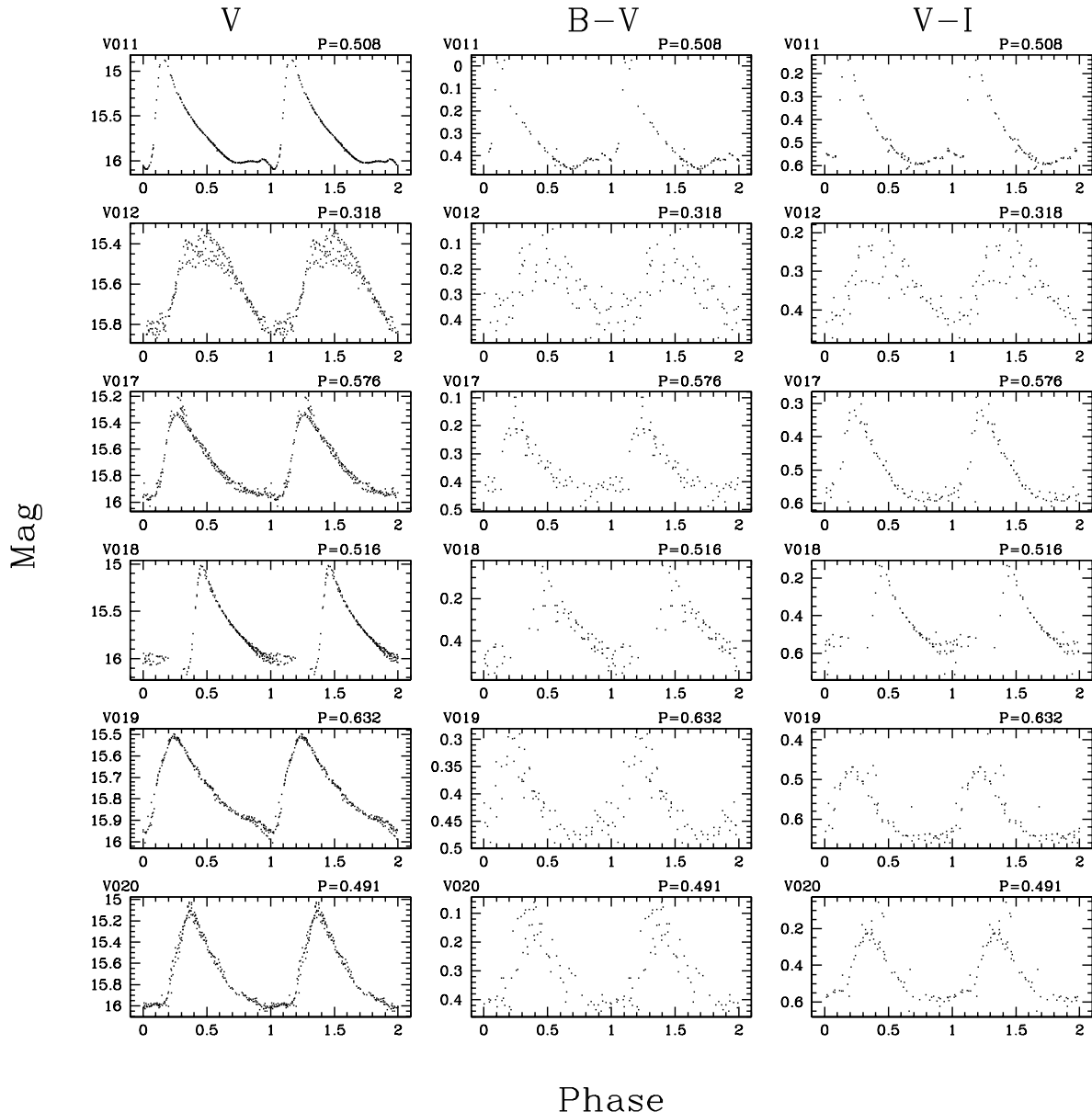


Fig. 5.— *Continued.*

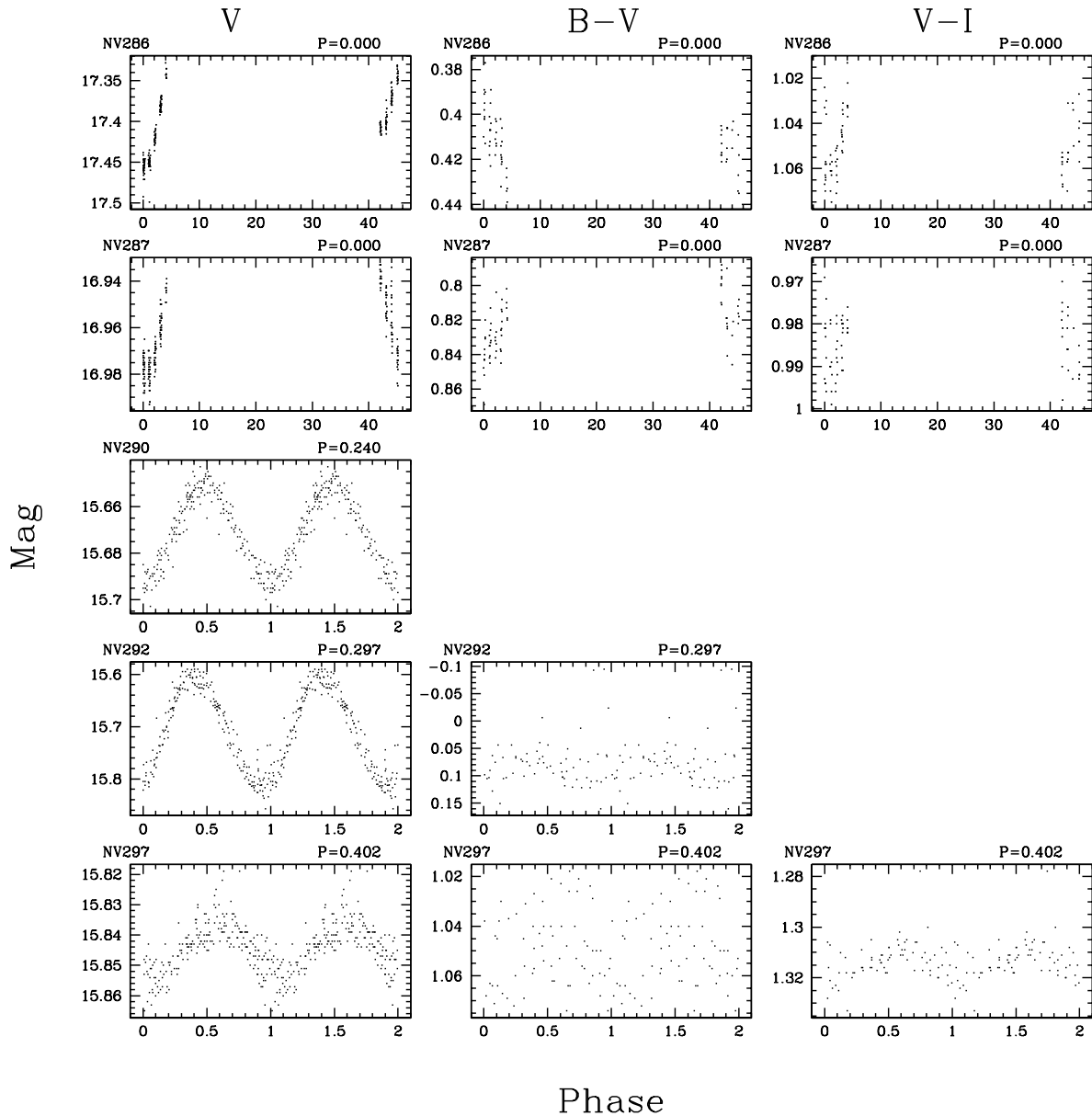


Fig. 6.— V , $B - V$, and $V - I$ light curves for the two new unclassified variables and the three newly discovered RR variables.

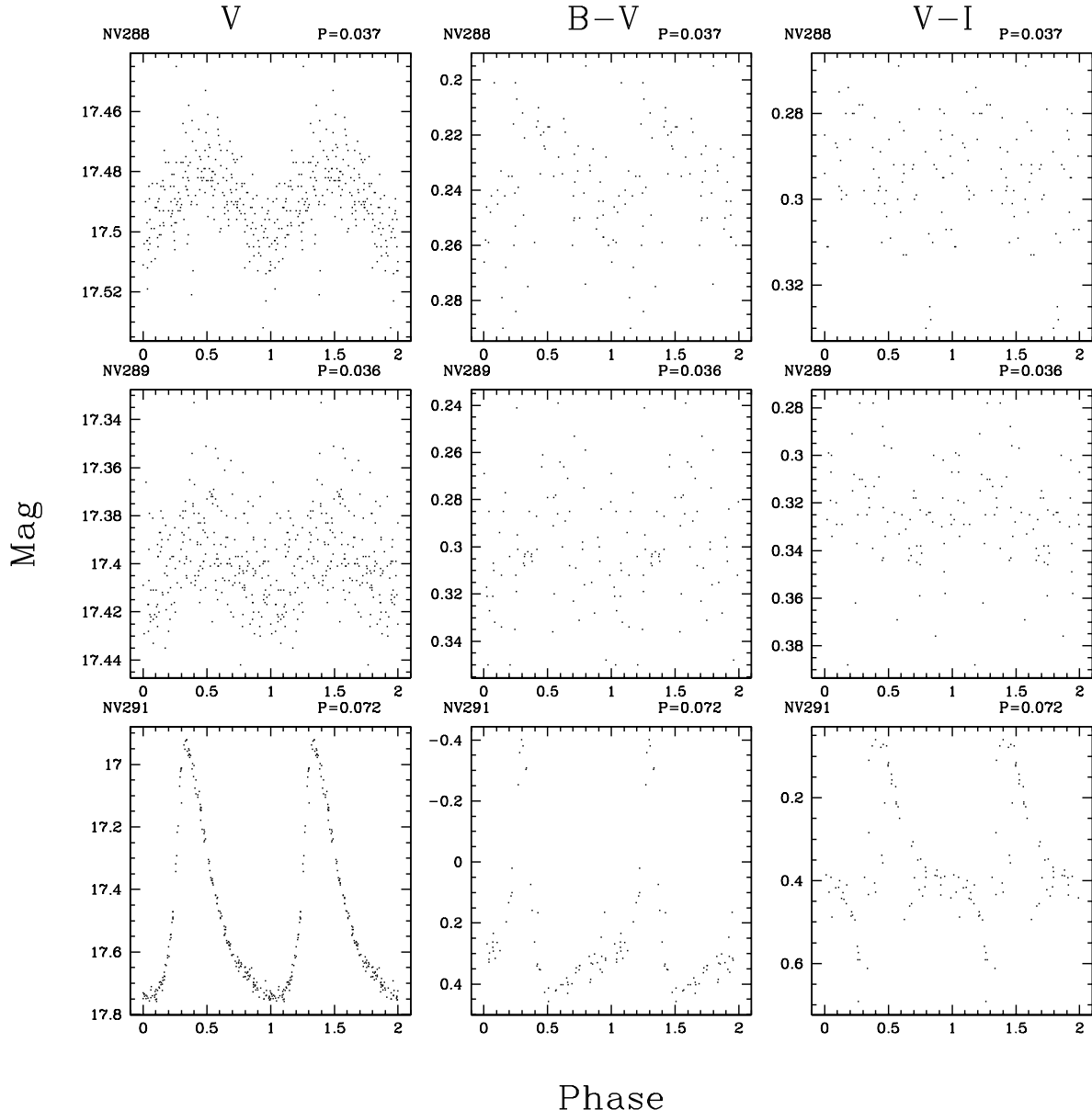


Fig. 7.— V , $B - V$, and $V - I$ light curves for the six newly discovered SX Phe type variables.

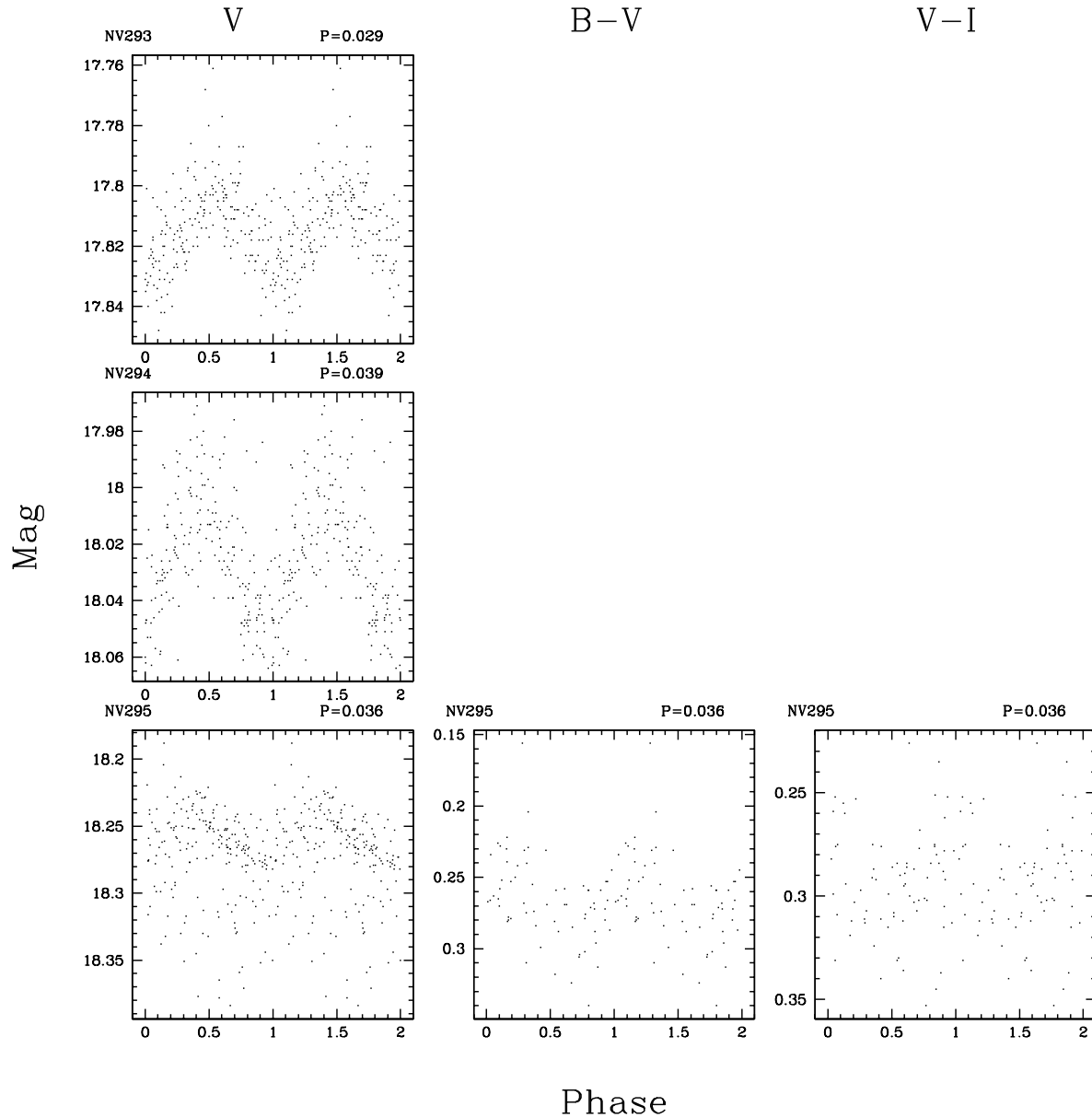


Fig. 7.— *Continued.*

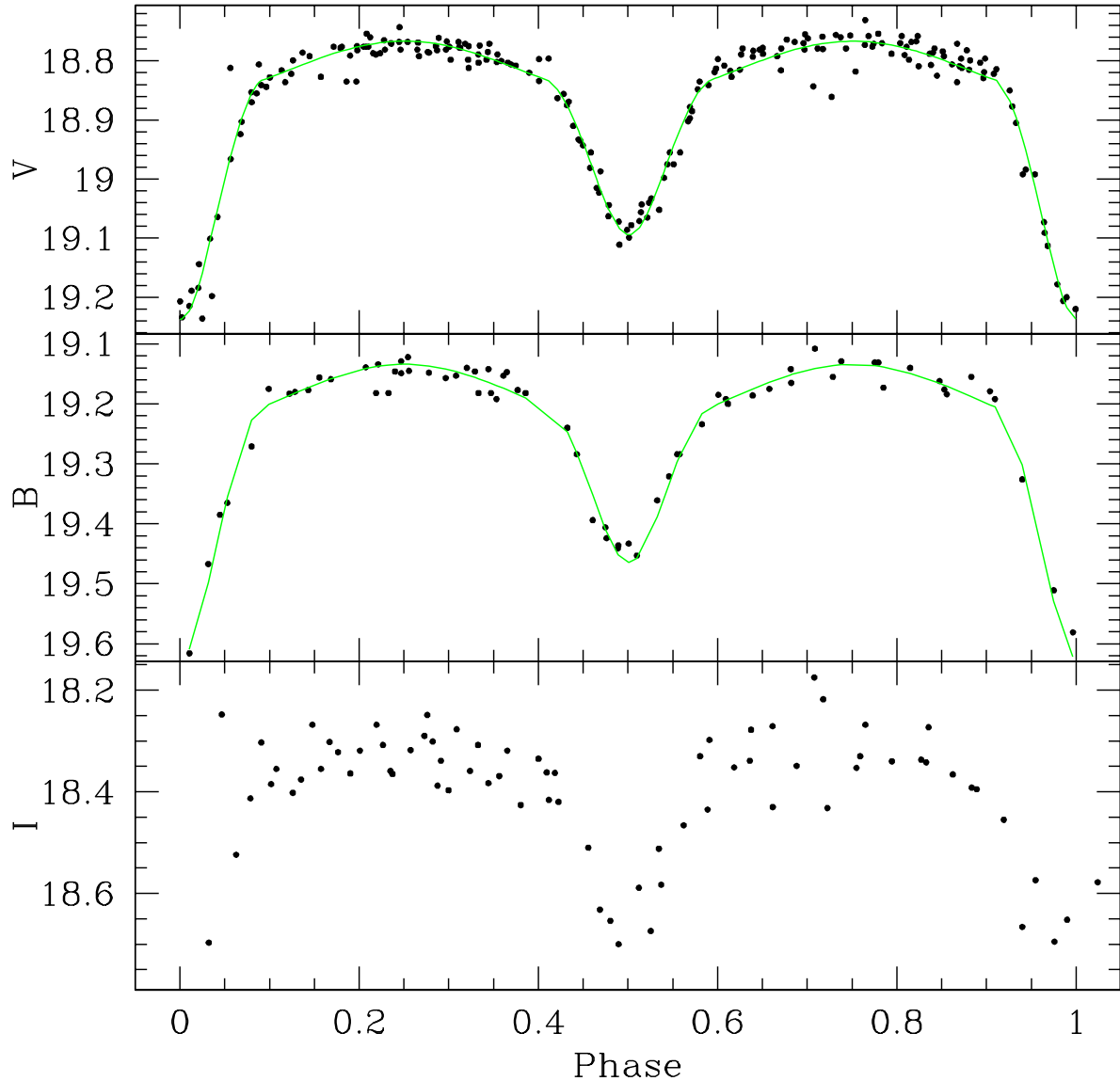


Fig. 8.— V , B and I -band light curves for the newly discovered eclipsing binary NV296. The solid line shows the model fit to the light curves using EBOP.

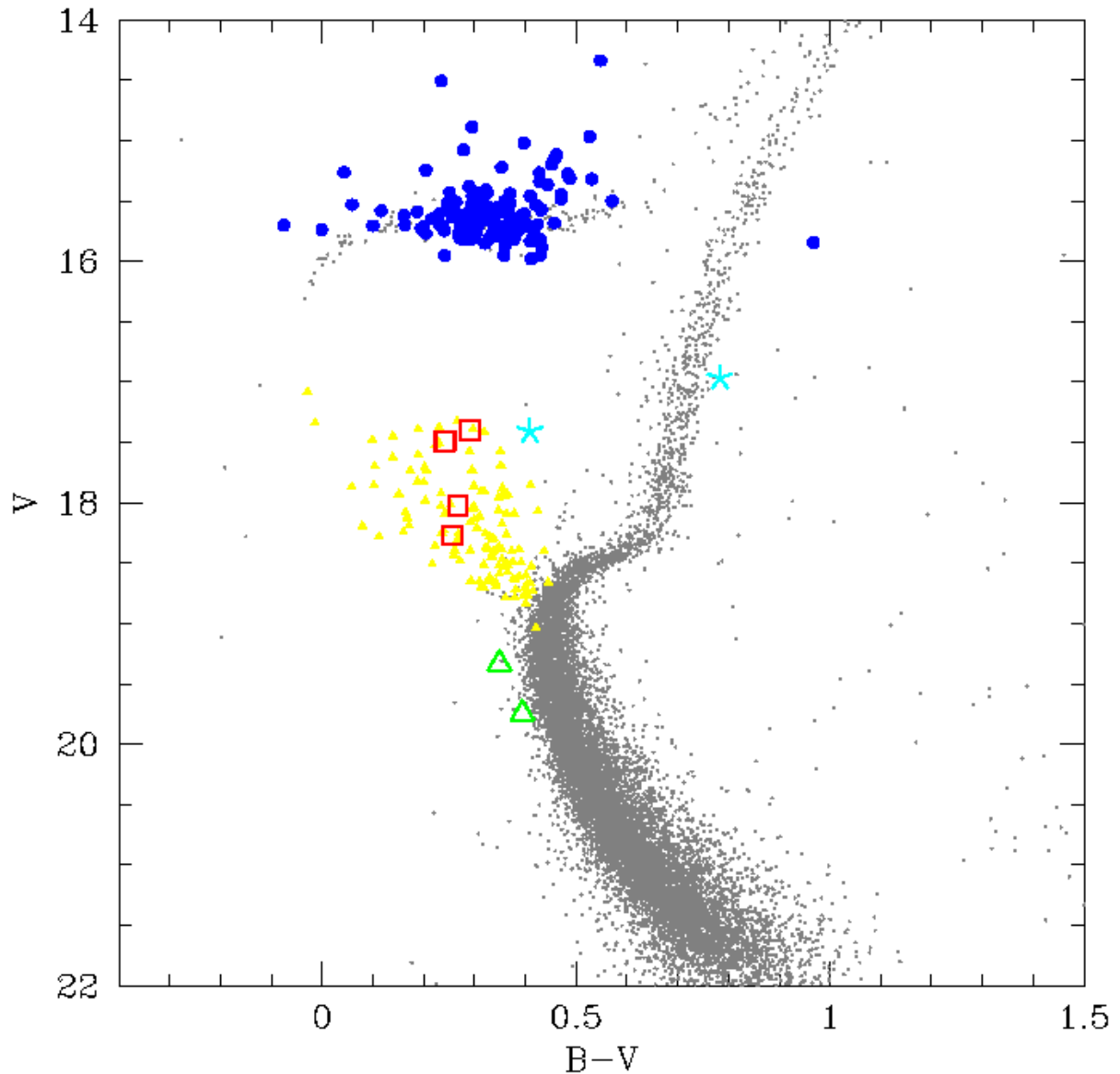


Fig. 9.— V vs $B - V$ CMD for M3. We use filled circles to show RR Lyr variables, open squares for SXP variables, stars for unclassified variables and open triangles for the two components of the EB. Filled triangles show the BSS stars that we examined for variability.

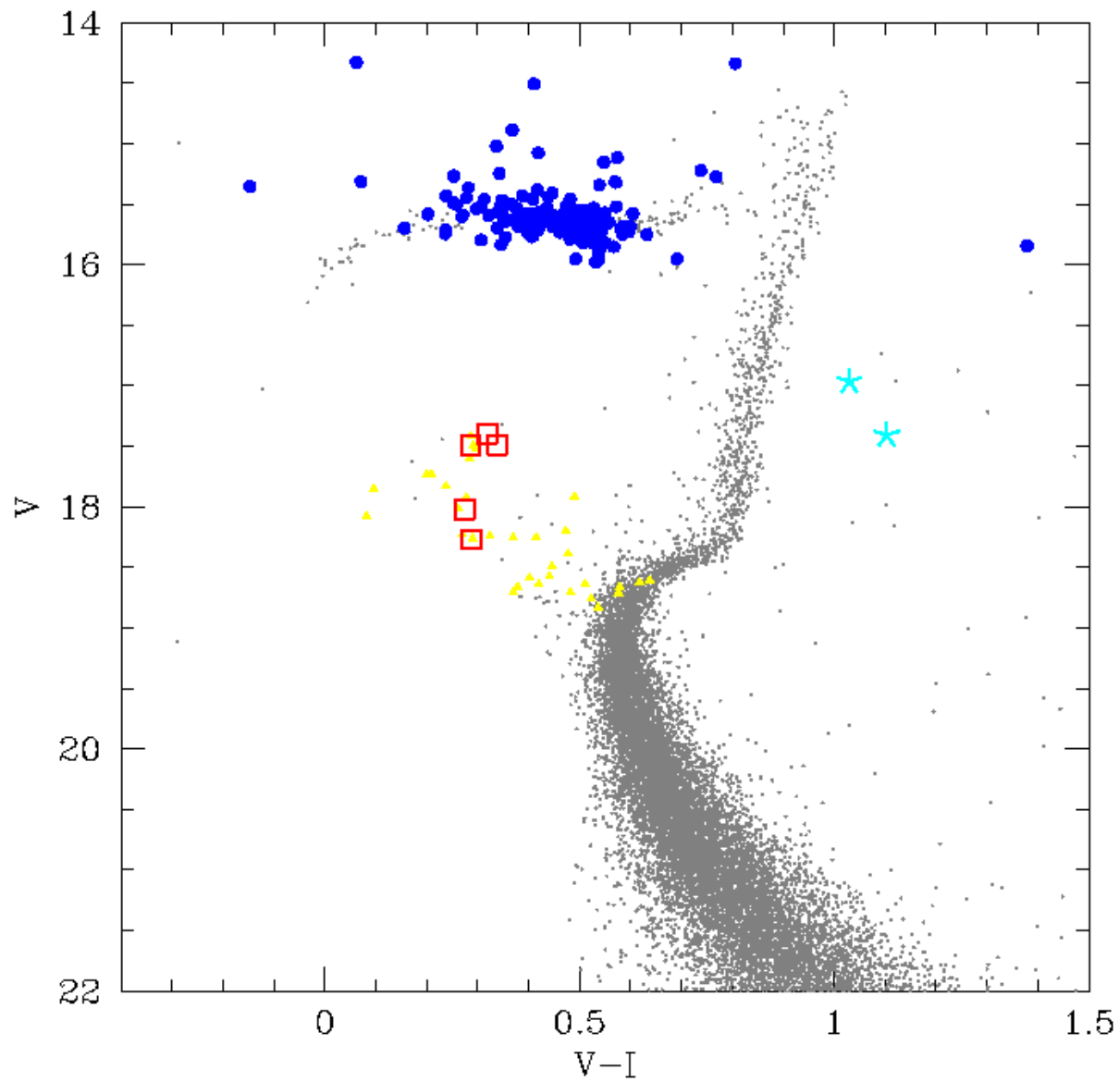


Fig. 10.— V vs $V - I$ CMD for M3. Symbols are as in Figure 9. The eclipsing binary is not shown on this diagram as we did not obtain a fit to the I-band light curve.

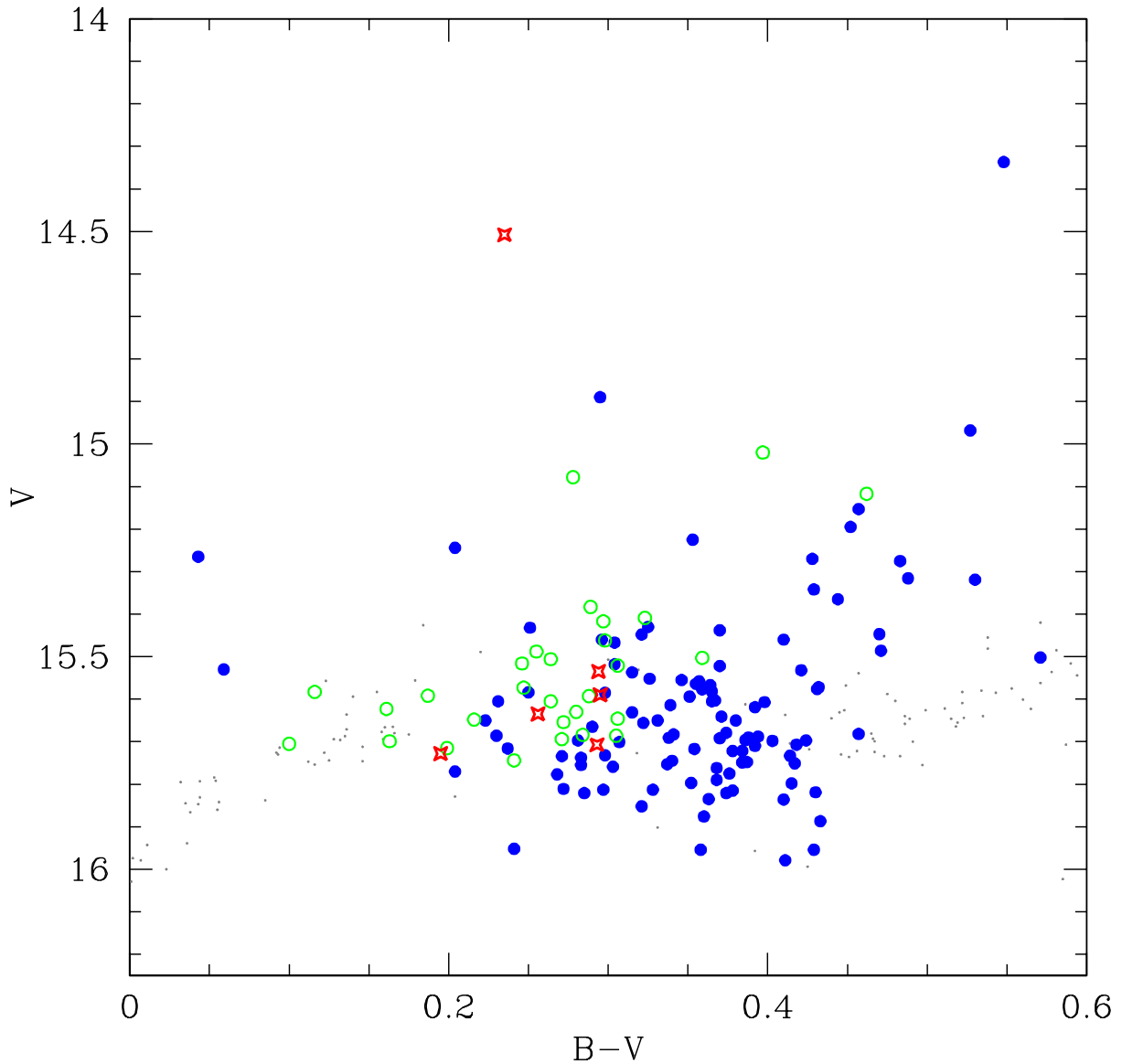


Fig. 11.— V vs $B - V$ CMD for the horizontal branch of M3. Here we distinguish between the types of RR Lyr variables using filled circles for RR0, open circles for RR1 and open stars for RR01 candidates.

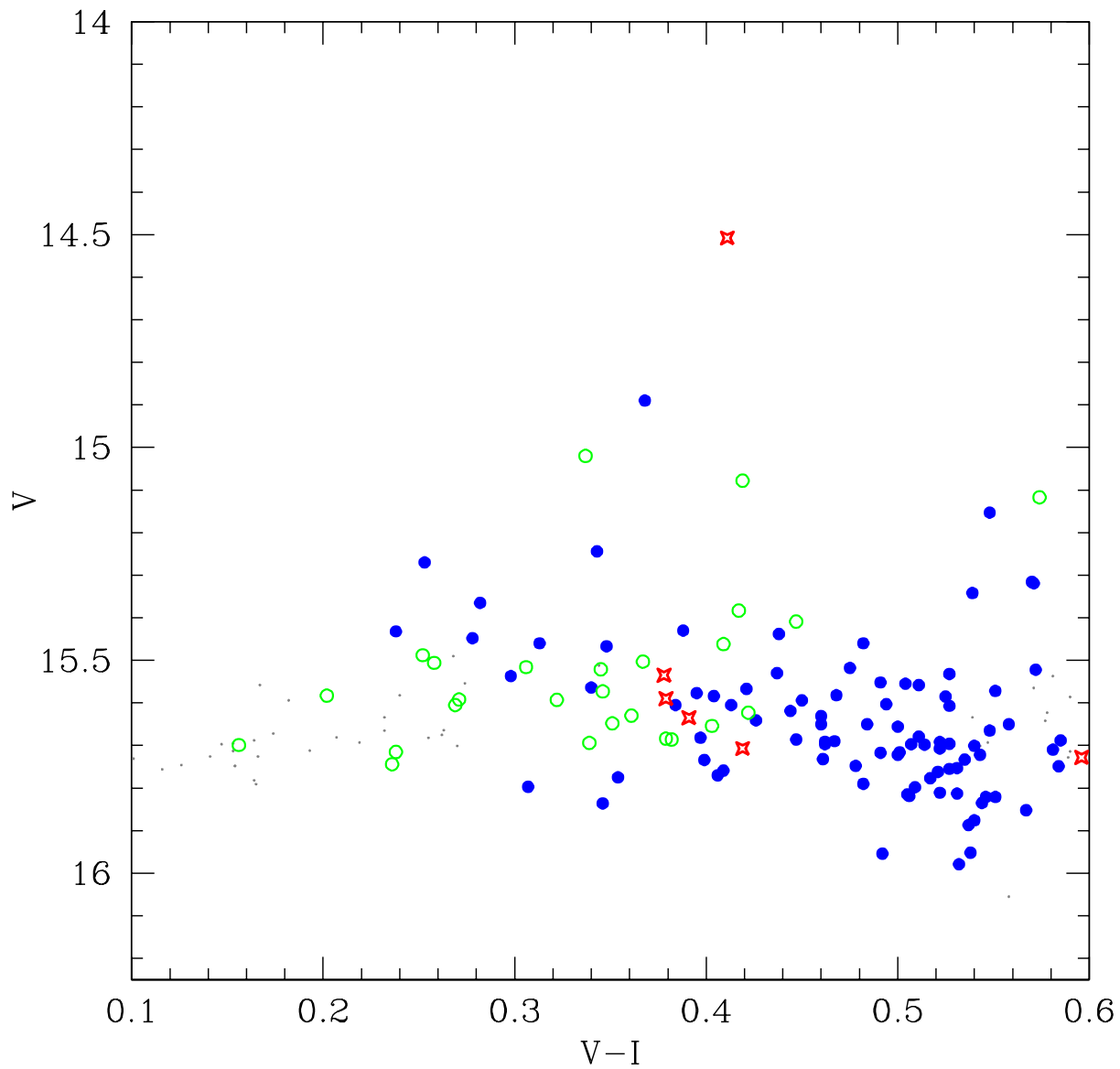


Fig. 12.— V vs $V - I$ CMD for the horizontal branch of M3. Symbols are as in Figure 11.

Table 1. Median Color of M3 Turnoff Stars

Chip	B-V	V-I
1	0.450	0.592
2	0.456	0.580
3	0.450	0.561
4	0.473	0.590

Table 2. EBOP Parameters for the EB NV296. Note that parameters for which the error listed is identical to zero were held fixed in the fitting process. All other errors are taken from the formal errors given by EBOP. The first two columns display results for a mass ratio of 1.0 the last two display the results for a mass ratio of 0.7. J_s and J_p is the surface brightness of the secondary and primary respectively, R_s is the radius of the secondary, and a is the semi-major axis.

Parameter	Value (q=1.0)	Standard Error	Value (q=0.7)	Standard Error
Mass Ratio	1.0	0.0	0.7	0.0
V Primary	19.331	0.028	19.351	0.024
V Secondary	19.747	0.042	19.719	0.036
(B-V) Primary	0.349	0.042	0.348	0.036
(B-V) Secondary	0.395	0.064	0.396	0.055
V J_s/J_p	0.65922	0.02325	0.64884	0.02280
B J_s/J_p	0.63197	0.03088	0.62028	0.02917
R_p/a	0.28594	0.00357	0.28499	0.00360
R_s/R_p	1.01456	0.02725	1.00764	0.02126
V Limb Darkening	0.57	0.00	0.57	0.00
B Limb Darkening	0.72	0.00	0.72	0.00
Inclination	75.66777°	0.50846°	75.86569°	0.47571°
Eccentricity	0.00	0.00	0.00	0.00
V Scale Factor	18.76666	0.00214	18.76719	0.00228
B Scale Factor	19.13395	0.00230	19.13484	0.00237

Table 3. Catalog of M3 Variables: First 12 Columns

ID	<i>2MASS</i>	α_{2000}	δ_{2000}	V_{flag}	B_{flag}	I_{flag}	A_V	$\langle V \rangle$	A_B	$\langle B \rangle$	A_I	$\langle I \rangle$
V001	1	13:42:11.12	+28:20:33.8	1	1	1	01.090	15.722	01.381	16.114	00.645	15.226
V004	1	13:42:08.21	+28:22:33.3	1	0	1	00.784	14.304	00.441	14.259
V005	1	13:42:31.29	+28:22:20.7	1	1	1	00.848	15.780	01.045	16.143	00.504	15.295
V006	1	13:42:02.08	+28:23:41.6	1	1	1	01.108	15.782	01.362	16.155	00.687	15.301
V007	0	13:42:11.09	+28:24:10.6	1	1	1	01.241	15.515	01.470	15.818	00.755	15.229
V009	1	13:41:49.51	+28:19:13.3	1	1	1	01.058	15.686	01.300	16.017	00.647	15.216
V010	1	13:42:23.10	+28:25:00.6	1	1	1	00.948	15.613	01.097	15.919	00.594	15.167
V011	1	13:41:59.98	+28:19:11.8	1	1	1	01.214	15.753	01.503	16.174	00.767	15.271
V012	1	13:42:11.26	+28:20:17.0	1	1	1	00.540	15.591	00.632	15.876	00.294	15.272
V017	1	13:42:22.42	+28:15:22.7	1	1	1	00.824	15.684	00.972	15.972	00.474	15.188
V018	1	13:42:18.95	+28:17:47.3	1	1	1	01.151	15.703	01.306	15.979	00.673	15.263
V019	1	13:42:38.12	+28:18:37.8	1	1	1	00.507	15.745	00.589	16.119	00.290	15.162
V020	1	13:42:36.83	+28:18:11.8	1	1	1	01.025	15.588	01.209	15.846	00.583	15.186
V021	1	13:42:37.78	+28:23:01.4	1	1	1	01.084	15.778	01.343	16.070	00.669	15.271
V022	1	13:42:25.92	+28:22:32.1	1	1	1	01.220	15.913	01.427	16.236	00.801	15.443
V023	1	13:42:02.84	+28:27:20.9	1	1	1	00.885	15.642	01.047	15.932	00.583	15.112
V024	1	13:42:00.31	+28:22:51.9	1	1	1	00.713	15.523	00.885	15.939	00.431	15.001
V027	1	13:42:03.17	+28:20:58.9	1	1	1	00.863	15.588	01.078	15.974	00.528	15.107
V030	0	13:42:08.73	+28:23:40.3	1	0	0	01.051	15.312
V031	1	13:42:13.97	+28:23:47.4	1	1	1	01.150	15.537	01.418	15.877	00.686	15.135
V032	1	13:42:12.39	+28:23:42.3	1	1	1	01.098	15.430	01.279	15.732	00.701	15.163
V034	1	13:42:21.71	+28:25:32.5	1	1	1	00.488	15.682	00.622	16.060	00.274	15.221
V036	1	13:42:24.55	+28:22:07.4	1	1	1	01.146	15.581	01.308	15.926	00.738	15.211
V037	1	13:41:53.56	+28:25:25.6	1	1	1	00.493	15.679	00.614	15.958	00.300	15.304
V038	1	13:41:56.04	+28:24:49.1	1	1	1	01.002	15.601	01.292	15.975	00.618	15.168
V039	1	13:41:52.97	+28:24:42.4	1	1	1	00.918	15.677	01.160	16.070	00.570	15.177
V040	1	13:41:50.93	+28:24:33.1	1	1	1	00.960	15.727	01.158	16.060	00.602	15.216
V043	1	13:42:19.07	+28:23:07.0	1	1	1	01.112	15.625	01.265	15.847	00.672	15.188
V044	1	13:42:24.37	+28:24:22.0	1	1	1	01.201	15.623	01.240	15.986	00.684	15.207
V045	1	13:41:53.23	+28:20:31.1	1	1	1	00.899	15.786	01.164	16.093	02.607	13.893
V050	1	13:42:12.24	+28:18:47.8	1	1	1	00.688	15.581	00.914	15.821	00.430	15.180
V051	1	13:42:13.87	+28:18:55.9	1	1	1	00.881	15.713	01.025	16.109	00.498	15.191
V053	0	13:42:10.94	+28:24:45.1	1	1	1	01.184	15.695	01.389	15.945	00.729	15.319
V054	1	13:42:08.98	+28:24:28.5	1	1	1	01.029	15.751	01.216	16.094	00.579	15.295
V055	1	13:41:55.91	+28:28:05.7	1	1	1	01.059	15.809	01.350	16.120	00.663	15.274
V056	1	13:42:00.67	+28:28:39.9	1	1	1	00.488	15.629	00.613	15.904	00.299	15.269
V057	1	13:42:23.25	+28:22:42.3	1	1	1	00.682	15.875	00.932	16.292	00.440	15.347
V059	1	13:42:03.25	+28:18:53.2	1	1	1	00.889	15.686	00.979	16.107	00.473	15.182
V060	1	13:41:49.05	+28:17:25.5	1	1	1	00.699	15.561	00.882	15.974	00.446	15.023
V061	1	13:42:25.78	+28:28:45.7	1	1	1	00.705	15.732	00.885	16.103	00.403	15.262
V062	1	13:42:18.22	+28:29:39.1	1	1	1	00.534	15.645	00.607	16.025	00.346	15.093

Table 3—Continued

ID	<i>2MASS</i>	α_{2000}	δ_{2000}	V_{flag}	B_{flag}	I_{flag}	A_V	$\langle V \rangle$	A_B	$\langle B \rangle$	A_I	$\langle I \rangle$
V063	1	13:42:14.21	+28:28:24.1	1	1	1	00.721	15.711	00.868	16.082	00.428	15.221
V064	1	13:42:20.11	+28:28:12.5	1	1	1	00.719	15.689	00.845	16.058	00.441	15.169
V065	1	13:42:20.92	+28:28:10.0	1	1	1	00.933	15.566	01.109	15.852	00.591	15.056
V066	1	13:42:03.77	+28:24:42.8	1	0	0	00.542	15.680
V067	1	13:42:01.51	+28:24:44.3	1	1	1	01.019	15.680	01.249	15.981	00.638	15.156
V068	1	13:42:13.09	+28:25:37.1	1	1	1	00.803	15.619	00.961	15.880	00.465	15.238
V069	1	13:42:17.57	+28:25:03.3	1	1	1	00.929	15.679	01.062	16.083	00.568	15.229
V070	1	13:42:14.32	+28:25:14.4	1	1	1	00.394	15.404	00.473	15.723	00.246	14.961
V071	1	13:42:23.65	+28:22:40.5	1	1	1	00.970	15.692	01.188	15.936	00.591	15.210
V072	1	13:42:45.25	+28:22:41.3	1	1	1	01.270	15.733	01.521	15.912	00.793	15.351
V073	1	13:42:44.72	+28:23:45.7	1	1	1	00.266	15.707	00.352	16.097	00.181	15.130
V074	1	13:42:18.15	+28:25:13.1	1	1	1	01.125	15.950	01.489	16.329	00.583	15.435
V075	1	13:42:15.13	+28:25:21.4	1	1	1	00.541	15.652	00.610	15.867	00.314	15.299
V078	1	13:42:15.06	+28:23:48.5	1	1	1	00.872	15.539	01.064	15.884	00.510	15.043
V079	1	13:42:14.69	+28:28:31.4	1	1	1	00.559	15.703	00.565	16.000	00.310	15.287
V080	1	13:42:43.02	+28:27:27.8	1	1	1	01.020	15.790	01.240	16.141	00.639	15.273
V081	1	13:42:37.36	+28:28:34.3	1	1	1	01.069	15.740	01.234	16.007	00.657	15.248
V083	1	13:41:38.00	+28:24:33.4	1	1	1	01.166	15.822	01.396	16.170	00.764	15.318
V084	1	13:42:16.31	+28:25:27.1	1	1	1	00.734	15.681	00.844	16.043	00.452	15.168
V085	1	13:42:34.65	+28:26:29.0	1	1	1	00.506	15.516	00.613	15.757	00.316	15.209
V087	1	13:42:19.84	+28:23:42.6	1	1	1	00.571	15.535	00.631	15.826	00.345	15.157
V090	1	13:42:18.92	+28:19:34.2	1	1	1	01.096	15.658	01.335	15.971	00.648	15.219
V091	0	13:42:10.59	+28:13:32.2	2	2	2
V093	1	13:41:47.40	+28:16:04.1	1	1	1	02.461	15.768	00.947	16.013	02.472	15.252
V094	1	13:41:34.54	+28:18:55.1	1	1	1	01.141	15.775	01.342	16.107	00.681	15.256
V096	1	13:41:59.12	+28:18:47.3	1	1	1	00.786	15.941	00.451	16.370	00.574	15.254
V097	1	13:42:01.70	+28:19:24.6	1	1	1	00.445	15.685	00.550	15.995	00.262	15.305
V099	1	13:42:26.76	+28:21:48.0	1	1	1	00.549	15.588	00.700	15.873	00.334	15.210
V100	1	13:42:16.75	+28:24:19.7	1	1	1	00.616	15.713	00.721	16.086	00.377	15.178
V101	1	13:42:14.98	+28:24:05.6	1	1	1	00.627	15.671	00.714	16.036	00.401	15.167
V104	1	13:42:09.49	+28:25:07.3	1	1	1	01.170	15.495	01.365	15.789	00.771	15.039
V105	1	13:42:09.85	+28:25:53.2	1	1	1	00.336	15.591	00.417	15.776	00.193	15.320
V108	1	13:41:54.77	+28:27:51.9	1	1	1	01.122	15.661	01.398	15.892	00.716	15.238
V117	1	13:42:18.39	+28:14:54.0	1	1	1	00.674	15.647	00.852	15.988	00.383	15.156
V118	1	13:42:22.50	+28:17:50.6	1	1	1	01.205	15.886	01.444	16.204	00.730	15.391
V119	1	13:42:30.67	+28:24:28.8	1	1	1	01.121	15.452	01.387	15.736	00.712	15.144
V120	1	13:41:48.99	+28:26:32.2	1	1	1	00.437	15.683	00.545	16.076	00.277	15.103
V121	0	13:42:08.17	+28:23:38.1	1	0	1	01.165	15.327	00.906	15.484
V122	0	13:42:09.03	+28:21:55.7	2	2	2
V125	1	13:42:25.64	+28:20:30.1	1	1	1	00.458	15.654	00.534	15.917	00.260	15.253
V128	0	13:42:20.12	+28:24:53.9	1	1	1	00.546	15.605	00.645	15.856	00.319	15.334

Table 3—Continued

ID	<i>2MASS</i>	α_{2000}	δ_{2000}	V_{flag}	B_{flag}	I_{flag}	A_V	$\langle V \rangle$	A_B	$\langle B \rangle$	A_I	$\langle I \rangle$
V129	0	13:42:08.21	+28:23:59.7	1	0	0	00.439	15.034
V130	1	13:42:11.77	+28:24:06.2	1	1	1	00.439	15.548	00.515	15.876	00.266	15.060
V134	0	13:42:09.78	+28:23:35.0	1	1	1	00.642	15.644	00.725	15.975	00.402	15.166
V135	1	13:42:09.43	+28:23:20.4	1	1	1	00.820	15.539	01.096	15.885	00.490	15.052
V136	0	13:42:09.57	+28:23:16.5	1	1	1	00.558	15.311	00.656	15.797	00.303	14.746
V137	1	13:42:15.47	+28:22:23.2	1	1	1	00.898	15.572	00.968	15.910	00.578	15.139
V139	0	13:42:14.11	+28:23:10.8	1	1	1	01.240	15.531	01.376	15.865	00.803	15.211
V140	1	13:42:10.28	+28:24:30.7	1	1	1	00.507	15.515	00.618	15.815	00.259	15.176
V142	1	13:42:09.26	+28:21:43.6	1	1	1	01.075	15.775	01.212	16.115	00.772	15.483
V143	1	13:42:08.88	+28:22:59.0	1	1	1	01.073	15.416	01.321	15.769	00.598	14.989
V145	0	13:42:13.61	+28:22:51.3	1	1	1	00.943	15.429	01.207	15.820	00.566	14.968
V146	0	13:42:18.48	+28:21:44.3	1	1	1	01.090	15.649	01.410	16.067	00.737	15.273
V147	0	13:42:09.83	+28:23:29.7	1	1	1	00.474	15.693	00.475	15.963	00.265	15.354
V148	1	13:42:10.95	+28:23:20.0	1	1	1	00.832	15.194	01.108	15.558	00.404	14.479
V149	0	13:42:14.10	+28:23:35.5	1	1	1	01.148	15.642	01.289	15.966	00.594	15.070
V150	0	13:42:16.68	+28:23:20.8	1	1	1	00.827	15.798	00.956	16.166	00.499	15.268
V151	0	13:42:11.99	+28:22:01.3	1	1	1	00.909	15.459	01.038	15.757	00.566	15.116
V152	1	13:42:17.47	+28:23:33.6	1	1	1	00.458	15.490	00.509	15.733	00.272	15.235
V156	0	13:42:09.99	+28:22:01.8	1	1	1	01.005	15.415	01.163	15.726	00.511	15.039
V157	1	13:42:10.20	+28:23:18.8	1	1	1	01.078	15.249	01.261	15.707	00.412	14.505
V159	0	13:42:10.34	+28:22:59.1	1	1	1	00.432	15.312	00.586	15.841	00.388	14.747
V160	0	13:42:10.80	+28:21:59.4	1	1	1	01.046	15.567	01.205	15.932	00.668	15.115
V161	0	13:42:12.80	+28:21:45.2	1	1	1	00.681	15.730	00.895	16.132	00.368	15.112
V165	0	13:42:17.04	+28:23:03.2	1	1	2	01.076	15.468	01.401	16.006
V168	1	13:42:08.09	+28:22:49.9	1	0	1	00.473	15.192	00.462	15.595
V170	1	13:42:09.33	+28:23:15.2	1	1	1	00.466	15.246	00.595	15.453	00.271	14.901
V171	0	13:42:09.51	+28:22:59.6	1	1	1	00.567	15.580	00.618	15.703	00.380	15.381
V172	0	13:42:09.89	+28:23:08.8	1	1	0	01.021	15.590	01.108	15.927
V173	0	13:42:10.50	+28:23:21.8	1	1	1	00.526	14.881	00.563	15.170	00.294	14.520
V174	0	13:42:10.84	+28:22:08.9	1	1	1	01.174	15.735	01.343	16.080	00.761	15.404
V175	0	13:42:14.62	+28:23:09.4	1	1	0	00.932	15.713	00.844	15.714
V176	0	13:42:14.98	+28:23:16.2	1	1	0	01.004	15.717	01.141	15.989
V177	1	13:42:16.28	+28:22:13.9	1	1	1	00.557	15.507	00.674	15.765	00.330	15.250
V178	0	13:42:17.47	+28:23:29.9	1	1	1	00.406	15.712	00.448	15.908	00.245	15.475
V180	0	13:42:10.09	+28:22:13.5	1	1	0	00.770	15.735	00.832	16.071
V181	0	13:42:09.21	+28:22:29.3	1	1	0	00.410	15.188	00.475	15.636
V184	0	13:42:09.57	+28:22:27.8	1	1	1	01.337	15.770	01.467	16.039	01.045	15.277
V187	0	13:42:09.64	+28:22:52.0	2	2	2
V188	0	13:42:09.49	+28:23:06.9	1	1	1	00.449	15.742	00.477	15.982	00.337	15.506
V189	0	13:42:09.59	+28:22:22.0	1	1	1	00.478	15.146	00.629	15.609	00.304	14.603
V190	0	13:42:10.88	+28:23:11.4	1	1	1	01.095	15.557	01.276	15.905	00.713	15.177

Table 3—Continued

ID	<i>2MASS</i>	α_{2000}	δ_{2000}	V_{flag}	B_{flag}	I_{flag}	A_V	$\langle V \rangle$	A_B	$\langle B \rangle$	A_I	$\langle I \rangle$
V191	0	13:42:11.60	+28:23:06.0	2	2	2
V192	0	13:42:11.31	+28:22:46.9	1	1	1	00.308	14.328	00.454	14.868	00.153	13.523
V193	0	13:42:12.61	+28:22:35.8	1	1	1	00.811	15.255	01.000	15.674	00.615	15.010
V194	0	13:42:12.74	+28:22:30.2	1	1	2	00.621	15.250	00.476	15.294
V195	0	13:42:10.48	+28:22:14.8	1	1	0	00.389	15.444	00.376	15.914
V197	0	13:42:15.91	+28:22:52.2	1	1	1	01.347	15.505	01.455	15.586	00.764	15.089
V200	0	13:42:11.19	+28:23:04.1	2	2	0
V201	0	13:42:11.78	+28:22:34.0	1	1	1	00.847	15.345	01.058	15.778	00.554	15.079
V202	1	13:41:42.83	+28:24:17.5	1	1	1	00.142	15.574	00.214	16.007	00.099	14.971
V207	1	13:42:14.19	+28:22:11.9	1	1	1	00.366	15.381	00.397	15.675	00.196	14.966
V208	0	13:42:11.72	+28:21:44.5	1	1	1	00.397	15.502	00.522	15.860	00.256	15.135
V212	0	13:42:09.87	+28:22:04.4	1	1	0	00.858	15.475	00.972	15.938
V213	0	13:42:09.57	+28:22:12.8	1	1	1	00.468	15.461	00.529	15.753	00.396	15.046
V214	0	13:42:13.94	+28:22:48.9	1	2	1	00.920	15.292	00.549	15.237
V215	0	13:42:10.43	+28:22:41.7	1	1	1	00.793	15.423	00.797	15.664	00.501	15.188
V216	0	13:42:13.60	+28:22:31.6	1	1	1	00.525	15.703	00.517	15.863	00.393	15.542
V218	0	13:42:13.62	+28:22:13.2	1	1	1	00.806	15.738	00.936	16.037	00.471	15.343
V220	1	13:42:13.98	+28:22:27.1	2	2	2
V221	0	13:42:10.21	+28:22:28.9	1	1	1	00.358	15.020	00.445	15.418	00.601	14.672
V223	0	13:42:13.28	+28:22:36.6	1	1	0	00.605	15.647	00.673	15.950
V229	0	13:42:09.00	+28:21:56.8	2	0	1	00.869	15.272
V234	0	13:42:13.09	+28:22:02.9	1	1	1	01.137	15.800	01.260	16.184	00.897	15.476
V235	0	13:42:13.77	+28:23:19.8	1	1	1	00.507	15.516	00.588	15.886	00.309	14.948
V237	0	13:42:15.73	+28:18:17.3	1	1	1	00.232	18.019	00.228	18.288	00.243	17.743
V239	0	13:42:09.86	+28:22:16.0	2	2	0
V240	0	13:42:09.46	+28:22:35.3	1	1	1	00.511	15.624	00.479	15.785	00.258	15.200
V241	0	13:42:10.76	+28:22:38.0	2	1	2	00.962	14.912
V243	0	13:42:12.25	+28:22:15.6	1	1	1	00.514	15.335	00.612	15.758	00.327	14.805
V245	0	13:42:09.89	+28:23:00.0	1	1	0	00.481	15.414	00.576	15.713
V246	0	13:42:12.76	+28:22:40.5	1	1	0	00.600	15.698	00.472	15.630
V247	0	13:42:14.81	+28:22:15.6	2	2	2
V249	0	13:42:10.31	+28:22:48.2	2	2	0
V250	0	13:42:10.51	+28:22:52.5	1	1	0	00.823	14.958	00.986	15.468
V252	0	13:42:10.99	+28:22:44.0	1	1	1	00.878	15.728	00.785	15.905	00.512	15.128
V253	0	13:42:12.14	+28:22:32.8	1	1	1	00.531	15.562	00.548	15.805	00.397	15.225
V254	0	13:42:12.42	+28:22:53.6	2	2	0
V255	0	13:42:12.62	+28:22:43.5	2	2	0
V256	1	13:42:13.08	+28:22:59.0	2	2	2
V258	0	13:42:14.31	+28:23:31.5	1	1	1	00.552	15.600	00.733	16.004	00.390	15.081
V259	0	13:42:14.57	+28:22:54.9	1	1	1	00.293	15.114	00.397	15.571	00.139	14.541
V261	0	13:42:10.08	+28:22:40.4	1	1	1	00.361	15.077	00.409	15.355	00.220	14.659

Table 3—Continued

ID	<i>2MASS</i>	α_{2000}	δ_{2000}	V_{flag}	B_{flag}	I_{flag}	A_V	$\langle V \rangle$	A_B	$\langle B \rangle$	A_I	$\langle I \rangle$
V264	0	13:42:10.87	+28:22:29.8	2	1	0	00.288	14.493
V269	0	13:42:12.79	+28:22:33.0	2	2	2
V270	1	13:42:11.93	+28:23:32.2	1	1	1	00.507	14.503	00.553	14.751	00.284	14.096
V271	1	13:42:12.16	+28:23:18.6	2	2	0
NV286	1	13:41:51.55	+28:17:00.6	1	1	1	00.171	17.406	00.104	17.816	00.128	16.304
NV287	1	13:41:41.00	+28:20:55.5	1	1	1	00.060	16.964	00.107	17.747	00.064	15.935
NV288	0	13:42:17.39	+28:13:35.1	1	1	1	00.087	17.489	00.079	17.731	00.051	17.204
NV289	1	13:42:12.17	+28:19:20.9	1	1	1	00.109	17.399	00.095	17.692	00.084	17.079
NV290	1	13:42:21.30	+28:23:45.0	1	0	0	00.060	15.670
NV291	0	13:42:18.07	+28:22:39.6	1	1	1	00.838	17.462	00.978	17.697	00.519	17.141
NV292	0	13:42:11.18	+28:21:54.0	1	1	0	00.267	15.704	00.251	15.809
NV293	0	13:42:20.59	+28:28:32.8	1	0	0	00.087	17.813
NV294	0	13:42:13.69	+28:25:30.3	1	0	0	00.093	18.024
NV295	0	13:41:58.56	+28:27:59.4	1	1	1	00.196	18.272	00.164	18.529	00.162	17.985
NV296	0	13:41:42.98	+28:24:04.0	1	1	1	00.466	18.767	00.310	19.134	00.398	18.307
NV297	1	13:41:31.72	+28:24:10.9	1	1	1	00.046	15.844	00.067	16.811	00.024	14.465

Note. — Full discussion of the column headings is presenting in §3 of the text.

Table 4. Catalog of M3 Variables: last 9 columns

ID	Per	Per _{pub}	Per _{flag}	JD _{min}	B _{phase}	I _{phase}	Class	Remarks
V001	0.520300	0.520596	0	920.705400	0.268883	0.305977	RR0	Bl?
V004	0.585033	0.584900	0	920.753434	...	0.109739	RR0	Bl?
V005	0.501451	0.504178	1	920.760300	0.107879	0.990228	RR0	Bl
V006	0.514333	0.514333	0	920.835834	0.672006	0.009527	RR0	
V007	0.497396	0.497429	0	920.866716	0.805403	0.974837	RR0	
V009	0.541545	0.541553	0	921.072365	0.006666	0.002899	RR0	
V010	0.569430	0.569544	0	920.748500	0.720984	0.048996	RR0	
V011	0.507910	0.507894	0	920.871500	0.999291	0.015948	RR0	
V012	0.317968	0.317540	1	920.737396	0.980589	0.070523	RR1	
V017	0.575998	0.576159	1	921.191002	0.066674	0.016840	RR0	Bl?
V018	0.516411	0.516451	0	920.928300	0.078831	0.072229	RR0	
V019	0.631976	0.631972	0	920.803000	0.001000	0.009766	RR0	Bl?
V020	0.491302	0.490476	1	920.785288	0.992062	0.130673	RR0	
V021	0.515786	0.515756	0	920.939100	0.286425	0.116502	RR0	
V022	0.481424	0.481424	0	920.986068	0.069577	0.987745	RR0	Bl
V023	0.595376	0.595376	0	920.942172	0.849769	0.016292	RR0	Bl
V024	0.663372	0.663372	0	920.808884	0.998667	0.022937	RR0	Bl
V027	0.579087	0.579073	0	921.214913	0.974076	0.988993	RR0	
V030	0.512092	0.512092	0	920.833332	RR0	
V031	0.580720	0.580720	0	921.008860	0.061716	0.013776	RR0	Bl?
V032	0.495350	0.495350	0	921.107500	0.791662	0.006258	RR0	
V034	0.559050	0.560963	1	920.860200	0.016725	0.130579	RR0	Bl
V036	0.545599	0.545599	0	921.000907	0.945748	0.981488	RR0	
V037	0.326639	0.326639	0	920.967091	0.056919	0.057786	RR1	
V038	0.558185	0.558011	0	921.025545	0.909089	0.891219	RR0	Bl?
V039	0.587067	0.587067	0	921.348533	0.002783	0.025438	RR0	
V040	0.551535	0.551535	0	920.761430	0.989919	0.030533	RR0	
V043	0.540532	0.540510	0	920.975472	0.053333	0.014800	RR0	
V044	0.506254	0.337850	0	920.924892	0.953762	0.037728	RR0	Bl
V045	0.536073	0.536073	0	920.886560	0.073397	0.672720	RR0	Bl
V050	0.512891	0.513170	1	921.143445	0.934918	0.994740	RR0	
V051	0.583970	0.583970	0	920.869800	0.993150	0.002654	RR0	Bl
V053	0.504881	0.504881	0	920.851000	0.969696	0.001218	RR0	
V054	0.506247	0.506247	0	920.804800	0.992703	0.943901	RR0	Bl?
V055	0.529822	0.529822	0	920.891956	0.994043	0.010203	RR0	
V056	0.329605	0.329600	0	920.839785	0.002670	0.065487	RR1	
V057	0.512191	0.512191	0	920.852656	0.979695	0.070478	RR0	
V059	0.588727	0.588826	0	921.113473	0.002257	0.989809	RR0	Bl
V060	0.707722	0.707727	0	921.270814	0.985164	0.000814	RR0	
V061	0.520941	0.520926	0	921.142959	0.958763	0.201435	RR0	Bl?
V062	0.652418	0.652418	0	921.309430	0.915695	0.075022	RR0	

Table 4—Continued

ID	Per	Per _{pub}	Per _{flag}	JD _{min}	B _{phase}	I _{phase}	Class	Remarks
V063	0.570282	0.570382	0	920.951790	0.009820	0.042435	RR0	
V064	0.605465	0.605465	0	921.317740	0.878928	0.005285	RR0	
V065	0.668349	0.668347	0	921.393302	0.987002	0.007501	RR0	
V066	0.620055	0.619100	1	921.305315	RR0	Bl
V067	0.568333	0.568333	0	921.186767	0.008622	0.996189	RR0	Bl
V068	0.358690	0.358690	0	920.998700	0.015612	0.077755	RR01	
V069	0.566615	0.566615	0	921.012215	0.938203	0.930535	RR0	
V070	0.486276	0.486093	1	921.023112	0.961314	0.101580	RR1	
V071	0.549053	0.549053	0	920.855294	0.865707	0.053314	RR0	Bl?
V072	0.456078	0.456078	0	920.761354	0.747315	0.986384	RR0	
V073	0.673659	0.670799	1	920.748500	0.982702	0.941698	RR0	Bl
V074	0.492152	0.492152	0	920.884772	0.988418	0.310481	RR0	
V075	0.314080	0.314080	0	920.860200	0.024134	0.885061	RR1	
V078	0.611965	0.611965	0	920.930100	0.936434	0.956615	RR0	Bl?
V079	0.361269	0.357269	1	921.049955	0.984222	0.990569	RR01	
V080	0.538331	0.537556	1	921.207445	0.995843	0.171571	RR0	Bl?
V081	0.529122	0.529122	0	921.025146	0.794478	0.053137	RR0	
V083	0.501264	0.501264	0	920.849544	0.728933	0.009289	RR0	
V084	0.595732	0.595732	0	920.923804	0.009400	0.990096	RR0	
V085	0.355808	0.355817	0	920.895076	0.989106	0.003541	RR1	
V087	0.354368	0.357478	0	921.064864	0.953427	0.078156	RR01	
V090	0.517031	0.517031	0	920.900000	0.036340	0.092138	RR0	
V091	0.529369	0.529369	0	920.829773	0.217140	0.168763	RR0	Bl?
V093	0.602294	0.602294	0	921.282644	0.746954	0.013283	RR0	Bl?
V094	0.523716	0.523696	0	920.813968	0.984251	0.962644	RR0	
V096	0.499416	0.499416	0	920.938568	0.061472	0.088704	RR0	
V097	0.334944	0.334933	0	920.805572	0.056224	0.055317	RR1	
V099	0.482199	0.361696	1	921.013804	0.914143	0.113858	RR01	Bl?
V100	0.618813	0.618813	0	920.813061	0.815114	0.005171	RR0	
V101	0.643886	0.643886	0	921.284314	0.967451	0.073370	RR0	Bl
V104	0.569946	0.569931	0	921.171862	0.989999	0.061220	RR0	
V105	0.287744	0.287744	0	921.001260	0.007187	0.058274	RR1	
V108	0.519615	0.519615	0	921.163810	0.987683	0.024586	RR0	
V117	0.600529	0.597263	1	921.078313	0.061159	0.028905	RR0	Bl?
V118	0.499391	0.499391	0	920.871036	0.014818	0.042051	RR0	
V119	0.517692	0.517692	0	921.188872	0.043431	0.994754	RR0	
V120	0.640139	0.640139	0	920.758900	0.917830	0.003601	RR0	
V121	0.535211	0.535211	0	921.211745	...	0.091366	RR0	Bl
V122	0.509621	0.516090	0	920.918108	0.274808	0.078937	RR0	
V125	0.349780	0.349823	0	920.924420	0.035165	0.998227	RR1	
V128	0.292044	0.292040	0	920.748500	0.869759	0.978962	RR1	

Table 4—Continued

ID	Per	Per _{pub}	Per _{flag}	JD _{min}	B _{phase}	I _{phase}	Class	Remarks
V129	0.406102	0.406102	0	920.957600	RR0	
V130	0.565181	0.567840	1	921.182519	0.897622	0.930886	RR0	Bl
V134	0.618057	0.618057	0	921.283896	0.015023	0.996254	RR0	
V135	0.568591	0.568397	0	921.171075	0.779662	0.978107	RR0	
V136	0.617153	0.617186	0	921.176847	0.031759	0.971968	RR0	
V137	0.575161	0.575161	0	921.070864	0.893209	0.887390	RR0	
V139	0.559970	0.559970	0	920.860200	0.007697	0.957783	RR0	
V140	0.333499	0.333499	0	920.813726	0.999409	0.121362	RR1	Bl?
V142	0.568628	0.568628	0	920.790800	0.023045	0.014069	RR0	
V143	0.596739	0.596535	0	921.340661	0.034987	0.019235	RR0	
V145	0.514456	0.514456	0	920.757864	0.733178	0.072504	RR0	
V146	0.502149	0.596745	1	920.939100	0.011152	0.934490	RR0	
V147	0.346495	0.346479	0	921.092130	0.000029	0.966839	RR1	
V148	0.467252	0.467290	0	920.988996	0.984154	0.016907	RR0	
V149	0.548252	0.548150	0	920.971600	0.966512	0.221876	RR0	
V150	0.523919	0.523919	0	920.811480	0.070358	0.156440	RR0	Bl
V151	0.516497	0.517767	1	921.141115	0.975617	0.018757	RR0	
V152	0.326130	0.326135	0	920.865910	0.017171	0.964094	RR1	
V156	0.532003	0.531987	0	921.113154	0.630164	0.956626	RR0	
V157	0.543086	0.542820	1	921.236948	0.064435	0.043076	RR0	
V159	0.534461	0.533260	1	921.009442	0.211989	0.118682	RR0	Bl?
V160	0.656928	0.657324	0	921.116672	0.022377	0.080551	RR0	
V161	0.526380	0.521640	1	921.221320	0.955925	0.073217	RR0	
V165	0.483630	0.483630	0	920.925300	0.980936	0.278767	RR0	
V168	0.274279	0.275970	1	920.865384	...	0.849482	RR1	
V170	0.432339	0.432260	0	921.088722	0.871899	0.978309	RR0	
V171	0.303307	0.303828	1	920.786330	0.965052	0.026376	RR1	
V172	0.542261	0.542288	0	920.859959	0.997274	...	RR0	
V173	0.607016	0.607016	0	921.186984	0.020296	0.103780	RR0	
V174	0.592278	0.587030	1	920.802710	0.829377	0.863071	RR0	Bl
V175	0.569703	0.569700	0	921.105385	0.958908	...	RR0	
V176	0.539702	0.540593	1	921.105838	0.066155	...	RR0	Bl?
V177	0.348338	0.348749	1	921.021524	0.931721	0.018993	RR1	
V178	0.266981	0.267387	1	920.748500	0.061053	0.025845	RR1	
V180	0.609131	0.615930	1	921.312176	0.010697	...	RR0	
V181	0.664073	0.663840	0	920.813281	0.075114	...	RR0	
V184	0.531176	0.532130	1	920.896900	0.852682	0.994819	RR0	
V187	0.585874	0.584126	1	921.311214	0.015553	0.952741	RR0	
V188	0.266510	0.266288	1	920.857460	0.983828	0.029642	RR1	
V189	0.612931	0.612940	0	920.984800	0.888405	0.869643	RR0	
V190	0.522735	0.522803	0	921.165465	0.639846	0.960018	RR0	

Table 4—Continued

ID	Per	Per_{pub}	Per_{flag}	JD_{min}	B_{phase}	I_{phase}	Class	Remarks
V191	0.525798	0.520030	1	920.770800	0.962122	0.308864	RR0	
V192	0.497111	0.497900	1	920.929278	0.017658	0.692467	RR0	
V193	0.747840	0.747840	0	920.970360	0.059104	0.059959	RR0	Bl?
V194	0.489200	0.489200	0	920.889000	0.848937	0.229967	RR0	
V195	0.643940	0.643940	0	920.898380	0.133118	...	RR0	Bl?
V197	0.499904	0.499904	0	920.764676	0.016379	0.016003	RR0	
V200	0.358013	0.359820	1	921.002184	0.970811	...	RR01	
V201	0.540571	0.541410	1	920.749258	0.917894	0.842581	RR0	Bl?
V202	0.773562	0.773562	0	921.023538	0.999889	0.074996	RR0	
V207	0.345329	0.344580	1	920.861604	0.042568	0.977804	RR1	
V208	0.338234	0.338020	0	920.898494	0.995867	0.961275	RR1	
V212	0.542136	0.542196	0	920.804712	0.977128	...	RR0	Bl?
V213	0.299944	0.299706	1	920.865036	0.002547	0.904996	RR1	
V214	0.539302	0.540450	1	921.266446	0.990758	0.232990	RR0	
V214	0.539489	0.540450	1	921.227229	RR0	
V215	0.528949	0.527100	1	921.184451	0.835527	0.892058	RR0	
V216	0.346484	0.346484	0	920.992228	0.956627	0.030443	RR1	
V218	0.544870	0.544870	0	920.770010	0.959623	0.864848	RR0	Bl
V220	0.600110	0.600110	0	920.975090	0.073636	0.096449	RR0	
V221	0.378752	0.378752	0	920.843884	0.118019	0.087656	RR1	
V223	0.329210	0.329586	1	920.855640	0.894201	...	RR1	
V229	0.503635	0.687700	1	920.978435	...	0.974515	RR0	
V234	0.507925	0.549500	1	920.785750	0.922823	0.900182	RR0	
V235	0.759901	0.765190	1	920.924695	0.978616	0.039742	RR0	Bl?
V237	0.041984	...	1	920.693148	0.209223	0.111185	SXP	mp
V239	0.497584	0.669490	1	921.034288	0.080003	...	RR0	
V240	0.276010	0.276010	0	921.004000	0.071012	0.135394	RR1	
V241	0.596172	0.594080	1	920.756216	0.766980	0.946418	RR0	
V243	0.634288	0.629910	1	921.108612	0.925611	0.947210	RR0	Bl?
V245	0.284037	0.284030	0	920.872941	0.858371	...	RR1	
V246	0.339171	0.339140	0	920.993319	0.032376	...	RR1	
V247	0.605350	0.605350	0	921.152200	0.010209	0.031635	RR0	
V249	0.533010	0.533010	0	921.201700	0.985666	...	RR0	Bl?
V250	0.590310	0.590310	0	920.847190	0.823415	...	RR0	Bl
V252	0.501550	0.501550	0	920.950300	0.855647	0.832519	RR01	
V253	0.332661	0.331610	1	920.850651	0.965971	0.931402	RR01	
V254	0.605519	0.604550	0	921.140032	0.873781	...	RR0	
V255	0.572640	0.572640	0	921.203710	0.651841	...	RR0	
V256	0.320459	0.318360	1	920.887774	0.945157	0.909177	RR1	
V258	0.713374	0.713409	0	921.050404	0.897383	0.981948	RR0	
V259	0.333463	0.332870	1	920.823344	0.037054	0.092532	RR1	

Table 4—Continued

ID	Per	Per_{pub}	Per_{flag}	JD_{min}	B_{phase}	I_{phase}	Class	Remarks
V261	0.444942	0.444140	1	920.945216	0.988843	0.972994	RR1	
V264	0.356490	0.356490	0	920.978930	0.903980	...	RR1	
V269	0.355657	0.290000	1	921.053598	0.902282	0.952330	RR1	
V270	0.690170	0.690170	0	921.052730	0.249736	0.178637	RR01	
V271	0.632472	0.630430	1	921.344022	0.004165	...	RR0	
NV286	0	N/A	
NV287	0	N/A	
NV288	0.036600	...	1	920.682300	0.147541	0.874317	SXP	mp
NV289	0.035789	...	1	920.703144	0.045321	0.296544	SXP	mp
NV290	0.240425	...	1	920.904200	RR01	
NV291	0.071629	...	1	920.770188	0.924779	0.940555	SXP	
NV292	0.296579	...	1	920.798310	0.887012	...	RR1	
NV293	0.029462	...	1	920.771768	SXP	
NV294	0.038827	...	1	920.781886	SXP	
NV295	0.036081	...	1	920.763793	0.842549	0.853940	SXP	
NV296	0.445955	...	1	921.127710	0.006637	0.950825	EB	
NV297	0.402037	...	1	920.948141	0.146715	0.748595	RR1	

Note. — Full discussion of the column headings is presenting in §3 of the text.